On Regional Characteristics of Seasonal Variation of Shallow Earthquake Activities in the World

AUTHOR(S):

MATSUMURA, Kazuo

CITATION:

MATSUMURA, Kazuo. On Regional Characteristics of Seasonal Variation of Shallow Earthquake Activities in the World. Bulletin of the Disaster Prevention Research Institute 1986, 36(2): 43-98

ISSUE DATE:

1986-06

URL:

http://hdl.handle.net/2433/124939

Bull. Disas. Prev. Res. Inst., Kyoto Univ., Vol. 36, Part 2, No. 318, June, 1986

On Regional Characteristics of Seasonal Variation of Shallow Earthquake Activities in the World

By Kazuo MATSUMURA

(Manuscript received January 31, 1986)

Abstract

Seasonality of earthquake occurrence and its relations to meteorological phenomena were investigated in respective seismic areas in the world. To do this, the worldwide data set by NOAA, a historical earthquake data set in China and Korea, and also a microearthquake data set in Japan were analyzed by the use of a point process analysis method recently developed by Ogata (1983).

By systematic and quantitative treatments, various characteristics of seasonality of earthquake occurrence were elucidated globally. Some areas showing clear seasonality of earthquake occurrence were found. Those areas are all situated in the middle latitude zone, and most of them are located in the intraplate seismic region just behind the active interplate seismic zone. On the other hand, seasonality of earthquake occurrence was not observed at all in oceanic regions and tropical regions.

Correlations between seasonal variation of seismic activity and variations of precipitation and of its change rate were high in the areas with clear seasonality. This phenomenon was explained by a triggering effect of groundwater which penetrated into cracks of the crustal rocks.

These results on seasonality of earthquake occurrence may give important material for investigations on earthquake mechanism and also on earthquake prediction.

1. Introduction

The temporal and spatial distribution of earthquake activity have been analyzed by many seismologists and various important characteristics are known today. One of the important results on the nature of seismic activity is that its seasonal variation has been found in some regions. Investigations on such seasonal characteristics of earthquake activity are found in some descriptions written by ancient philosophers. Their descriptions were briefly introduced by Tributsch (1978).[1)]

The first seismologist who reported on such a nature was Omori (1902)[2)]. He found annual periodicity of small earthquake activity from his observation. Davison (1928)[3)] studied the data of earthquake occurrences in many regions throughout the world and concluded that the peaks of monthly distribution of earthquakes in the Northern and the Southern Hemispheres occur in the same season.

On earthquakes of large magnitude in and around Japan, Mogi (1969)[4)] studied their annual distribution, and showed that they have a peak in a limited season and the season is different between adjacent active zones. Large earthquakes in the region along the Japan trench from Hokkaido to Sanriku occurred during the season from February to May. Most large earthquakes occurred in March. In the adjacent region along the coast line from Miyagi to Shikoku, annual distribution of large earthquakes ($M \geqq 7.5$) has a peak in December.

There exist some results on similar seasonal characteristics of microseismicity. For example, Oike (1977)[5] described that monthly distribution of shallow microearthquakes in the Inner Zone of Southwest Japan shows a similar pattern to the rate of changing of monthly mean precipitation. In this region the same nature of seasonality was found not only on microearthquakes but also on medium magnitude earthquakes from JMA data and large disastrous earthquakes from historical data. He showed that microearthquake activity along the Yamasaki fault in this region clearly increases closely related to rainfall and also indicated many cases where heavy rainfall can be a trigger to the occurrence of earthquakes.

Close relations between seismicity and precipitation or water level of the river have been discovered in many places throughout the world. McGinnis (1963)[6] investigated the relation between the shallow earthquake activity in New Madrid in Missouri and the water level of the Mississippi. He showed that the monthly distribution of earthquakes has a similar pattern to the changing rate of the monthly mean water level.

In Japan, Ozawa (1968 and 1969)[7,8] reported that change of strain by heavy rainfall is related to the occurrence of small shallow earthquakes. Yamauchi (1981)[9] calculated strain responses to precipitation by tank model, and found out that earthquakes occurred before and after the abnormal strain responses to rainfall.

There are some important results concerning the relation between groundwater and occurrence of shallow earthquakes. One of them is a result of the reservoir induced earthquakes. Drastic change of water level in a dam often gives rise to occurrence of earthquakes. This problem has been investigated since 1945 (Carder, 1945)[10]. Talwani (1976)[11] observed the increase of seismic activity 46 hours after a rapid ascent of water level in the dam by a heavy rainfall. Gupta and Rastogi (1976)[12] summarized the data concerning induced earthquakes associated with large reservoirs. Induced seismicity at the 315 m-high Nurek dam in Tadjikistan, USSR were investigated by Simpson and Negmatullaev (1981)[13] and Keith et al (1982)[14]. They showed that the seismicity was related to rapid increases in water level up to 105 m in 1972 and to 205 m in 1976. Oike and Ishikawa (1983)[15] studied the reservoir induced earthquakes in China and showed that the maximum magnitude of the induced earthquakes is related with the dam height. They showed that some large aftershocks of the Xinfengjiang earthquakes were induced by loading and unloading.

Ohtake (1974)[16] made an important experimental study in the Matsushiro swarm region. He indicated that a series of microearthquakes occurred two to four kilometers away from the well into which water was injected with a pumping pressure of 50 to 14 bars. A series of microearthquakes commenced several days after the start of water injection.

These phenomena mentioned above show that water injection into fractured zones could trigger earthquakes, probably due to the decrease of strength of rocks in the region.

In the active fault zone where stress level in the crust is critical, variations of small external stresses may become a trigger to the occurrence of earthquakes. Various kinds of phenomena such as earth tide, ocean tide and others are reported to be able to act as triggers. This suggests that seasonal variation of some kind of meteorological phenomena may also be a trigger to occurrence of earthquakes under a certain critical condition.

On the other hand, statistical analyses have been carried on for the annual change of earthquake activity. Ogata (1983)[17] analyzed the temporal distribution of earthquakes in the Inner Zone of Southwest Japan, applying point processes model with linearly parameterized intensity, and found that it has a similar pattern to an increasing rate of precipitation. He described the process where a drastic change of rainfall in the typhoon season or after the dry season can be a trigger of earthquakes.

He also analyzed the temporal distribution of earthquakes in Australia (Ogata and Katsura, 1986)[18]. The seasonal variation of seismicity in an area of Capital Territory a similarity to the rainfall pattern in Sydney. He suggested that in this case the drastic change of groundwater migration can be a trigger.

However, such characteristics of seismicity have not been investigated by fully systematic and quantitative analyses and by the use of the worldwide and long-term seismological data.

The present author has collected and edited many kinds of seismicity data for statistical analyses. These are considered qualified for systematic and quantitative investigations of seismicity mentioned above, and it will provide important information to clarify the mechanism of earthquake occurrence. If the seasonal variation of shallow earthquakes is the proper nature in a certain region, quantitative analysis of the temporal distribution of earthquakes is also useful for earthquake prediction study.

In this paper we shall analyze the temporal distribution of activity of shallow earthquakes in all active regions in the world using the long-term seismicity data above-mentioned. The new statistical point process analysis proposed by Ogata (1983)[17] is applied to them, and characteristics of the seasonal variation of earthquakes and moreover mechanisms of such phenomena will be discussed.

2. Data of seismicity used for the study

There are many kinds of data set available for the analysis of seismicity. In order to investigate the seasonal variation of seismic activity, a data set must consist of fairly long-term and homogeneous data. The worldwide epicentral data sets have been published by The National Geophysical Data Center of The National Oceanic and Atmospheric Administration (NOAA). Two data sets by NOAA have been used, in the present study, for the analysis on the nature of all regions in the world. One was published in 1973 and the other in 1981.

The former consists of 86,069 events from January, 1900 through May, 1973. The latter 113,592 events span from January 1928 through May 1981. These two data sets have been used for the analysis of activity for two periods from January, 1900, to May, 1973 and from June, 1973 to May, 1981, respectively. These data sets are uniform through the periods for the earthquakes with magnitudes greater than 7.0 all over the world. Through the period from 1928 to 1981 they are uniform for the earthquakes with magnitudes greater than 6.5. Almost all earthquakes with magnitudes greater than 5.0 have been observed all over the world since 1961.

Only shallow earthquakes with depths less than 40 km are analyzed in this study, because deep earthquakes are considered to be less influenced by seasonal effects.

Some special long-term data sets have been used to analyze seismicity in detail especially of the East Asia region. In China, historical earthquake data have been compiled by the Institute of Geophysics, the Chinese Academy. A list of strong earthquakes with magnitudes greater than or equal to 6.0 is used in this analysis. This list was edited from the Catalogue of Chinese Earthquakes which was published by the Institute of Geophysics. It includes 686 earthquakes since B.C. 780 to A.D. 1977. The Catalogue of Chinese Earthquakes edited by Gu et al (1983) is also used. It must be the longest historical data of inland earthquakes in the world. 1394 earthquakes with magnitudes greater than 4 which have been surveyed by seismologists and historians in China are listed up since B.C. 1177 to A.D. 1949.

Historical data of comparatively large earthquakes in Japan are also used for the analysis of seismicity in and around Japan. Disastrous earthquakes in Japan have been studied and listed up by Usami (1975)[19] since 416 to 1973. They are also published in the Rika Nenpyo every year, and 421 earthquakes since 427 to 1978 were described in the list published in 1981.

Kim and Suh (1977)[20] studied and listed up earthquakes in Korean Peninsula and compiled historical data since A.D. 27 to 1977. In their list magnitudes of earthquakes were not determined but only intensities in JMA scale were reported. In Korea the seismic activity is comparatively low and the magnitude of earthquakes is not so large. The maximum intensity on their list is 5. The list consists of 61 earthquakes since A.D. 27 to 1727 and 382 earthquakes since 1905 to 1977.

The Korean Peninsula is located between Northeastern China and Southwest Japan where large earthquakes occur in the active fault regions. The data file in Korea by Kim and Suh is used for the analyses to clarify the nature of seismicity in the region between these two active regions.

Seismological data which has been compiled by the Tottori Microearthquake Observatory, Disaster Prevention Research Institute, Kyoto University from June 1965 to March 1985 are used for the detailed analysis of microearthquakes in the Inner Zone of Southwest Japan. In this region many active faults have been found from geological survey and seismological observation, and the relations between

microearthquakes and active faults have been studied from various viewpoints.

One of the important phenomena to be compared with results of seasonality of seismicity is the annual distribution of precipitation in the region concerned. It is suggested by Oike (1977)[5] and Ogata (1983)[17] that there is a close relation between the seasonal distribution of microearthquakes and the variation of the precipitation in the Yamasaki fault region.

To examine such characteristics in various regions, worldwide data of precipitation are required. Hourly or daily data of precipitation are not available in almost all regions of the world. But the data sets of monthly mean precipitation are available all over the world from the Rika Nenpyo. The latter is rather suitable than hourly or daily data of precipitation to compare with the analyzed results of seasonal variations of seismic activity, because both of the data are considered to show smoothed patterns.

In some regions precipitation does not always mean rainfall, but it may consist only of snow in winter. For some cold regions where rainfall data are not available, data sets of temperature from the Rika Nenpyo are also referred to.

3. Method of statistical analysis of seasonality

The quantitative analysis and estimation of seasonal variation of seismic activity are the main themes in this paper. The best method of statistical analysis must be chosen for that purpose. It is an important problem to calculate intensity or amplitude of seasonal variation in time series of earthquakes and to know the pattern of seasonal distribution concerning the probability of earthquake occurrence. And it is also important to choose the best fitting model, quantitatively.

The occurrence of an earthquake is not a continuous phenomenon. Earthquakes are described by points in space and time. The method of analysis suitable for our purpose must be able to process such data described by points. The point process analysis which was developed by Ogata (1986)[18] was adopted as the best method of analysis in this study.

Such analyses have been applied in order to know the characteristics of seismicity, especially its seasonality in various regions of the world. It has now been made possible by the recent development of the high speed computer with high density memories.

One method of estimation of unknown parameters is the method of the maximum likelihood. The statistical model whose parameters maximize the likelihood are adopted as the best one by this method. In general, the larger the number of parameters is, the larger the likelihood becomes. Then the question comes how many parameters should be adopted for the best estimation of the statistical model. Akaike (1973)[21] proposed the Akaike Information Criterion (AIC) as the universal criterion for estimating the model. AIC is defined by

$$\mathrm{AIC} = (-2)\max(\log \text{likelihood}) + 2(\text{number of parameters}) \qquad (1)$$

where log denotes the natural logarithm. The model with the smaller AIC shows a better fitness to the data. The second term in (1) is larger when the number of parameters is larger. This shows that for estimation it is important to find the model in which the number of parameters becomes as few as possible. The method of minimizing AIC is now used in various fields for estimation of a statistical model.

Ogata (1986)[18] applied the maximum likelihood analysis of point process to seismological data. In the present paper the temporal distribution of shallow earthquakes have been analyzed on the basis of the point process models, following.

The variation of seismic activity involves many frequency components. Extremely low frequencies are called a trend, while moderate frequencies corresponds to annual, semi-annual, seasonal, monthly or daily effects. High frequencies indicate clustering effects such as aftershocks, foreshocks and earthquake swarms. The model suggested by Ogata (1986) takes the following form,

$$\lambda_\theta(t\,|\,F) = a_0 + P_J(t) + C_K(t) + \sum_{t_1<t} g(t-t_1)\,. \tag{2}$$

The first and second terms correspond to the seismic trend, the third and fourth terms correspond to the periodic and clustering effects, respectively. Those components are represented as follow;

$$P_J(t) = \sum_{j=1}^{J} a_j \phi_j(t)\,, \qquad 0<t<T \tag{3}$$

$$C_K(t) = \sum_{k=1}^{K} \{b_{2k-1}\cos(2k\pi t/T_0) + b_{2k}\sin(2k\pi t/T_0)\}\,, \tag{4}$$

$$g_M(t) = \sum_{m=1}^{M} c_m X^{m-1} e^{-\alpha K}\,. \tag{5}$$

T in eq. (3) is the total length of the observation period and $\phi_j(t)$ is a polynomial of order j. T_0 in eq. (4) is a fixed period for certain periodic effects. As the seasonal variation of seismic activity is treated in this paper, T_0 is fixed as 365.24 days. In this case $k=1$ means the annual variation, $k=2$ means semi-annual and so on. If the scaling parameter α is fixed, model described eq. (2) is linearly parameterized by eq. (3), (4) and (5).

The existence of each component, especially the seasonal variation, is examined quantitatively and the shape of the seasonal distribution of seismic activity is calculated by this model.

The parameter estimation is formed by maximizing L,

$$\log L = \sum_{i=1}^{I} \log \lambda_\theta(t_i\,|\,F_{t_i}) - \int_0^T \lambda_\theta(t\,|\,F_t)\,dt\,, \tag{6}$$

To find the best model among those with feasible combinations and their orders, the Akaike Information Criterion AIC has been adopted.

We need much time to calculate AIC for high orders of a triplet of all components, J, K, M in eq. (3), (4) and (5). To save time the fourth term in eq. (2) which

corresponds to the clustering effect is omitted in view of the result of the preliminary analyses. **Fig. 1** shows the fourth term in eq. (2) in the Alaska area. In this case, clustering effects are observed about ten days after a shock. In several other cases which have been calculated preliminarily, clustering effects last less than ten days and almost all the clustering effects are extinguished within five days. Therefore, the earthquake which occurred within five days after the previous one will not be counted to remove the clustering effect. We calculated in the case where the orders of the second and third terms, J and K, are 0 to 4.

For better understanding the results in this paper two concrete examples are presented. One is the case where seasonal variation of seismic activity exists (**Fig. 2**, **Fig. 3** and **Table 1**), and another the case where it does not exist (**Fig. 4**, **Fig. 5** and **Table 2**).

The left side of **Fig. 2** indicates the distribution of the monthly number of shallow earthquakes with magnitudes greater than or equal to 5.0 in the Alaska area (A4), as shown in **Fig. 7**. It reveals a tendency for higher activity around June in this region. Our purpose is to analyze this tendency quantitatively. The right side of **Fig. 2** shows the time series of the occurrence of shocks. The total number of earthquakes is 58 and the total length of interval is 27,978 days from January 1,

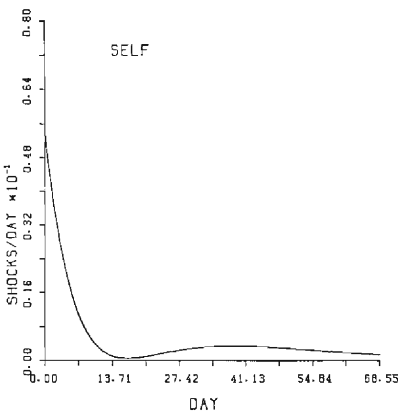

Fig. 1 An example of self exciting components, as seen in the fourth term in eq. (2), of earthquakes in A4 area.

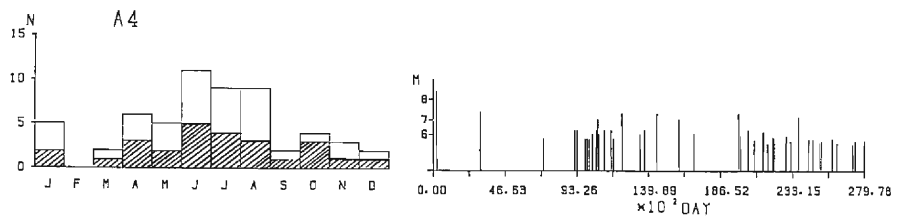

Fig. 2 Monthly distribution (left) and time series (right) of earthquakes ($M \geqq 5.0$) in the Alaska area (A4). The hacthed areas in the left figure indicate the numbers of earthquakes with $M \geqq 6.0$.

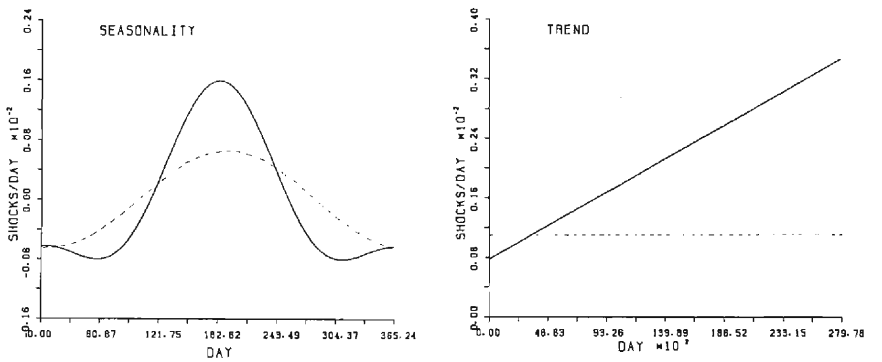

Fig. 3 Seasonal (left) and trend (right) components calculated by the best fitting model in Alaska area (A4). The solid and dotted lines correspond to the components in the cases with the thresholds of magnitudes 5.0 and 6.0, respectively.

Table 1 AIC calculated for various cases in the Alaska area (A4). In the case where that the order of trend component J=1 and that of seasonal component K=2, AIC is of minimum value. This indicated the best fitting model.

K \ J	0	1	2	3	4
0	834.73	824.86	826.70	828.49	829.92
1	825.64	818.33	820.14	821.88	823.15
2	825.18	817.48	819.36	819.69	821.58
3	827.84	821.18	823.08	823.61	825.51
4	828.43	824.37	826.28	826.96	828.88

1940 to August 8, 1980.

AIC is calculated for 25 cases in which the orders of the trend and seasonal components are fixed independently from 0 to 4 as shown in Table 1. AIC becomes the smallest as seen in the Table, when the orders of the trend (J) and seasonal component (K) are 1 and 2, respectively. J=1 means that the linear increment of seismicity which is caused by untraced small earthquakes in earlier years of the 20th century exists. The trend is displayed by a right-upward line as shown in **Fig. 3**. K=2 means that annual and semi-annual seasonal variations exist. The seasonal pattern consists of large annual and small semi-annual components, as shown in **Fig. 3**.

Fig. 4 shows the monthly distribution of earthquakes in the Gulf of the Alaska area (A2), shown in **Fig. 7**, with magnitudes greater than or equal to 6.0. It shows no particular seasonal tendency. **Table 2** shows the calculated AIC values for various models. In the case of J=1 and K=0, it takes a minimum value. As mentioned above, J=1 means that linear increment exists, as shown in **Fig. 5**. K=0 means that no seasonal components exist in the seismic activity in the A2 area.

In these two cases, AIC becomes smallest independently of J value. For more than 80% cases of this analysis, AIC takes the smallest value independently of J

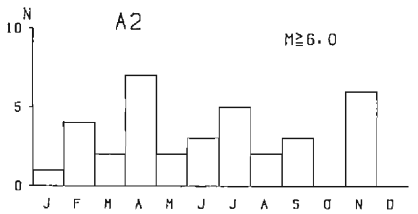

Fig. 4 Monthly distribution of earthquakes (M≧6.0) in the Gulf of the Alaska area (A2).

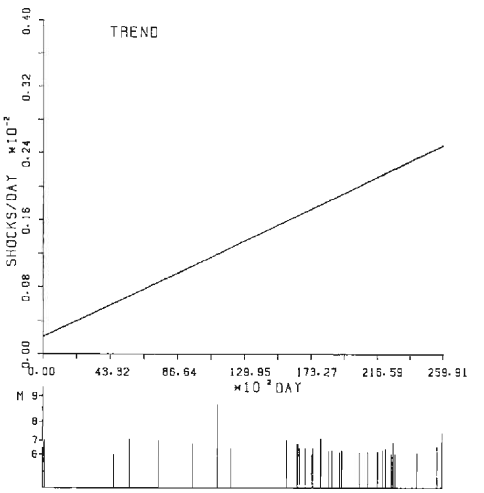

Fig. 5 Trend component calculated by the best fitting model in the Gulf of the Alaska area (A2). Time series of earthquakes is also shown in the lower portion.

Table 2 AIC of earthquakes in the Gulf of the Alaska area (A2). When J=1 and K=0, AIC is minimum. K=0 means that no seasonal components exist and J=1 means that either linear increment or decrement of seismicities exists.

K \ J	0	1	2	3	4
0	534.71	524.39	524.82	525.89	527.85
1	535.91	525.53	525.08	526.22	527.70
2	538.96	528.22	527.02	528.47	530.20
3	534.14	532.12	530.81	532.35	534.03
4	537.69	536.00	534.59	535.91	537.84

value. This suggests that the seasonal variations could be detected even if the detection capability would not be uniform in time.

We need large computer memory and much time to calculate AIC for a large number of earthquakes, hence the number of earthquakes had to be limited to less than 100 for an area as a rule. The lower limit of the number is taken to be 20. On this condition, we calculated AIC for various thresholds of magnitudes of earthquakes. For example, four cases are examined in the Alaska area (A4). For thresholds of magnitudes 4.5, 5.0, 5.5 and 6.0, the numbers of earthquakes are 122, 58, 42 and 26, respectively. In the case when the threshold of magnitudes is 4.5, the same seasonal variation has been detected as in the case when the threshold of magnitudes is 5.0. In two cases when the thresholds of magnitudes are 5.5 and 6.0, AIC took a minimum value for K=1. The best fitted models do not have semi-annual components which are shown in the former two cases. The peak of annual components in the cases of M 5.5 and M 6.0, however, correspond to the larger

peak in the former two cases for K=2. The annual component in the case with the threshold of magnitudes 6.0 is shown by a dotted line in the left side of **Fig. 3**, comparing with that in the case of M 5.0.

The results of these analyses are too many to be shown in this paper, so almost all of them will be described briefly. Tables of AIC for the areas whose monthly distribution of earthquakes are shown in this paper are listed up in Appendix.

4. Result in each region

To clarify the regional characteristics of seismicity the worldwide data of NOAA were used. Preliminary division was made referring mainly to the tectonic boundaries and the pattern of the spatial distribution of epicenters, on the condition that the size of each divided area be smaller than 500 square km. In the next stage, we examined the monthly distribution of earthquakes with various thresholds of magnitudes in each of the areas, and then rearrangements were made for the areas where the number of earthquakes with $M \geqq 5.0$ is smaller than 20 or that with $M \geqq 6.0$ is larger than 100. Finally seismically active regions in the world were divided into 96 areas as shown in **Fig. 6**. The results of analysis in each area will be described in the following sections, 4.1 to 4.11.

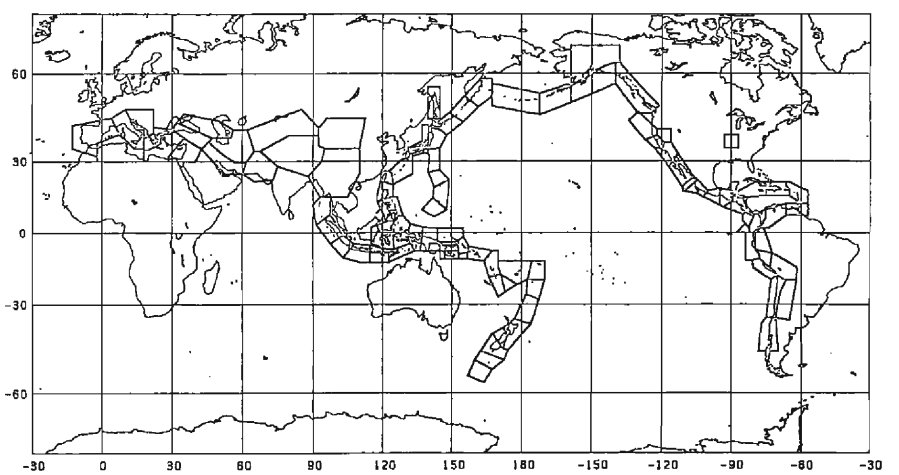

Fig. 6 Division of areas investigated on seasonality using NOAA's data.

4.1 Alaska and eastern Aleutian region

In the region from the Aleutian islands to the west coast of Canada through the Alaskan peninsula a lot of earthquakes have occurred. In the Alaska area, earthquakes in the crust are widely distributed by compressional stress fields caused by relative movements between the Pacific and North American plates. This region is divided into four areas (A1, A2, A3 and A4), as shown in **Fig. 7**. Results of analysis for shallow earthquakes in three areas, namely, along the Aleutian

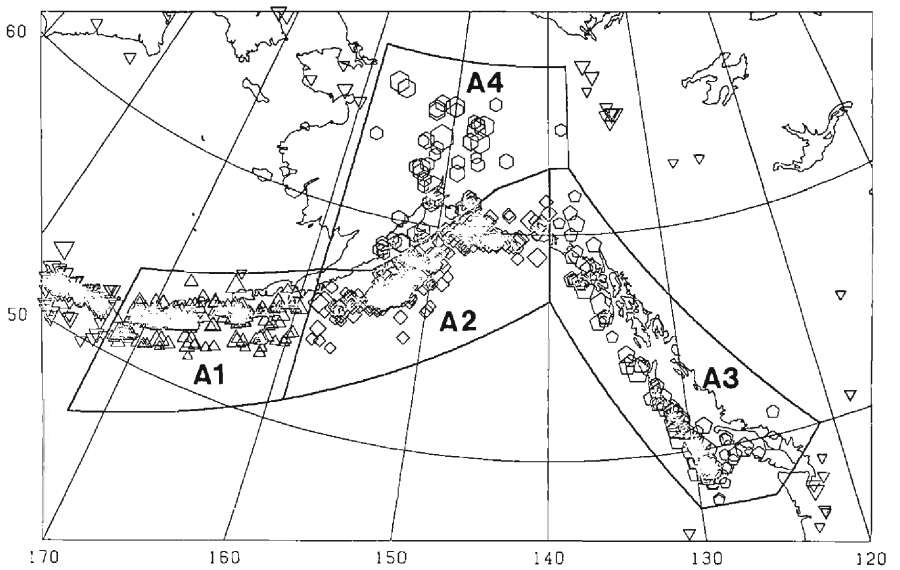

Fig. 7 Epicentral distribution of earthquakes ($M \geqq 5.0$) in the Alaska and eastern Aleutian region. A1, A2, A3 and A4 indicate the area number used in the text.

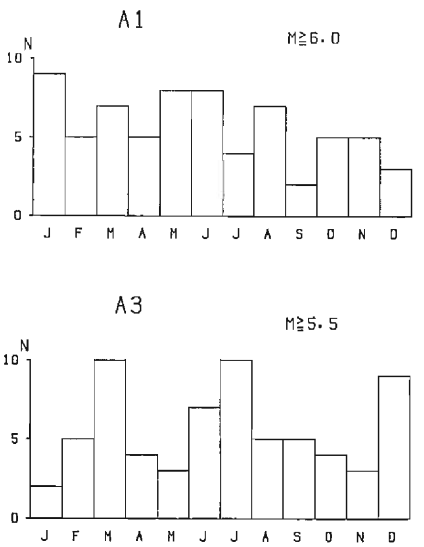

Fig. 8 Monthly distribution of earthquakes in the A2 and A3 areas.

islands (A1), along the coast of the Alaskan peninsula (A2) and along the west coast of Canada (A3), show no significant seasonal variations of seismicity, as explained by **Fig. 4**, **Fig. 5** and **Table 2** in the previous chapter.

Only the result of shallow earthquakes which occurred in the inland part of the Alaskan Peninsula (A4) shows a periodic variation of seismicity, as also explained by **Figs. 2** and **3** in the previous chapter.

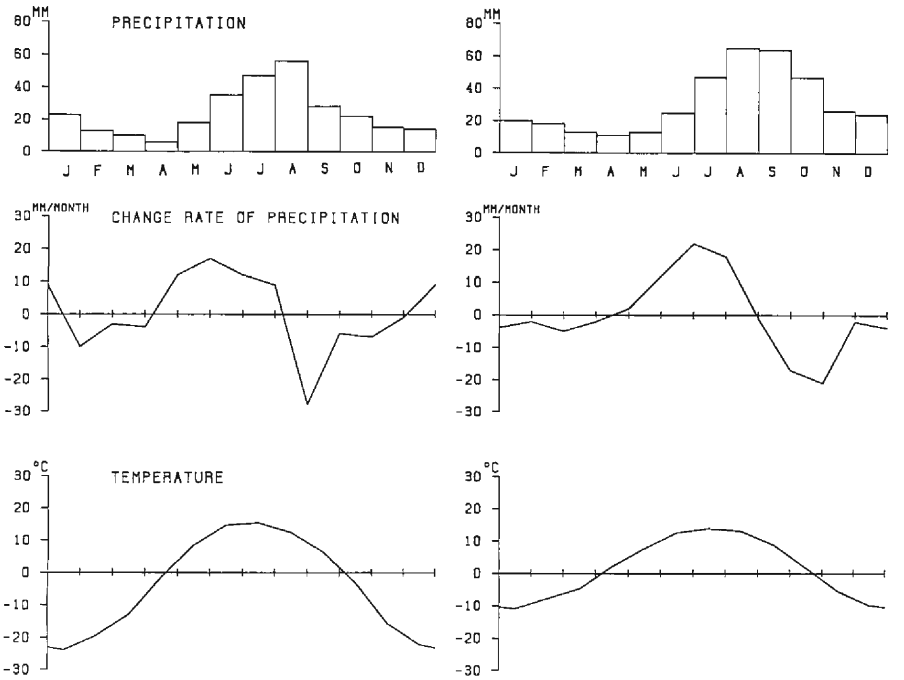

Fig. 9 Monthly mean precipitations, its change rate and temperature in the Alaska area. The left and right sides correspond to Fairbanks and Anchorage, respectively.

Distributions of monthly mean precipitation and of its increasing rate are shown in **Fig. 9**, with that of temperature. The right figures are those at Fairbanks in central Alaska and the left ones at Anchorage in the south part of Alaska. Since the temperatures at these two cities are below 0°C in the winter season from September to March, as seen in **Fig. 9**, the precipitation in this season may not correspond to rainfall, but to snow. Therefore, the monthly mean temperatures were examined to make up this disadvantage in the winter.

The pattern of the monthly distribution of precipitation is not similar to that of earthquakes. The peak of the monthly distribution of earthquakes in **Fig. 2** is in June and is about two months earlier than that of precipitation. It corresponds to the season when the change rate of precipitation is highest and also to the season just after the temperature goes up over the melting point, as shown in **Fig. 9**.

4.2 North America region

Fig. 10 shows the epicentral distribution of shallow earthquakes with magnitudes greater than or equal to 5.0. The west coast of North America is divided into six areas (B1 to B6). Earthquakes in the northernmost area (B1) have a periodic pattern of distribution. On the other hand, no seasonal pattern is found in the B2, B3, B4 and B5 areas. Monthly distributions of earthquakes with magnitudes greater

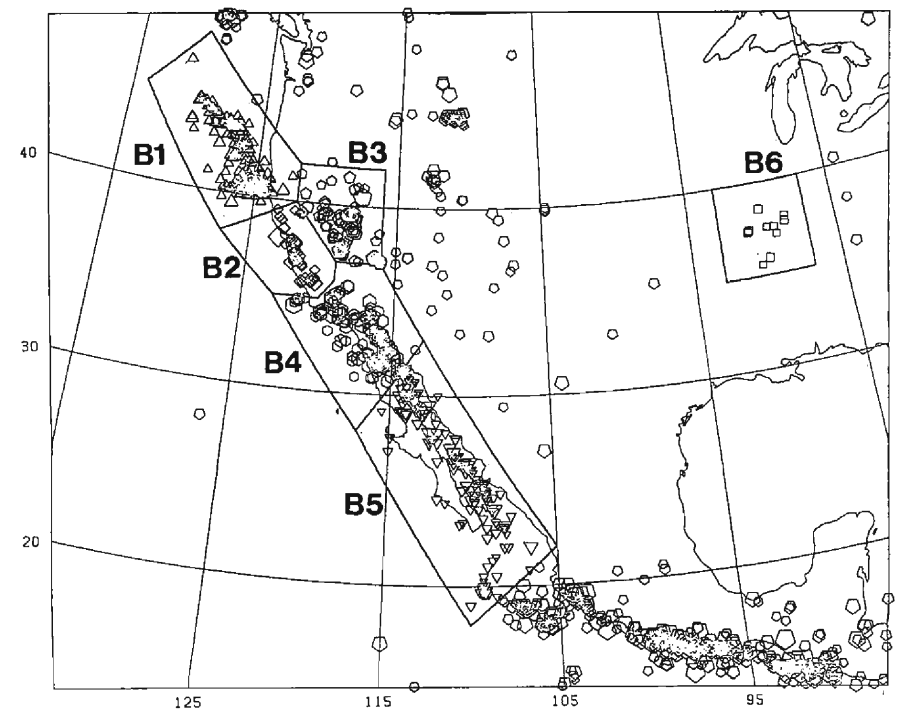

Fig. 10 Epicentral distribution of earthquakes (M≧5.0) in the North America region, and its division into 6 areas.

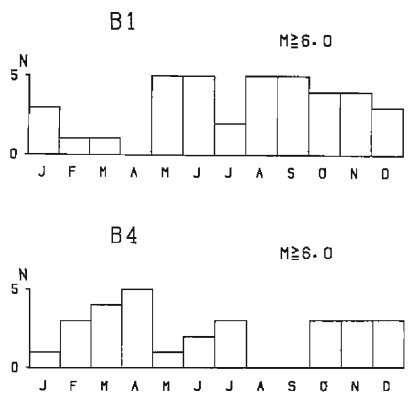

Fig. 11 Monthly distribution of earthquakes (M≧6.0) in the B1 and B4 areas.

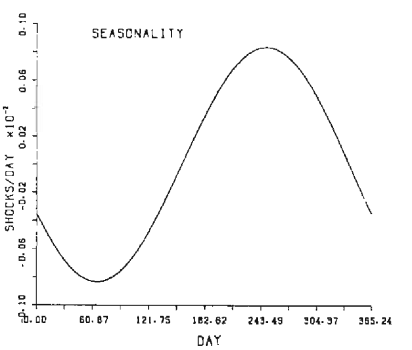

Fig. 12 Seasonal components of the best fitting model of the B1 area.

than or equal to 6.0 in the B1 and B4 are shown in **Fig. 11** as two typical examples. **Fig. 12** shows the result of analysis in the B1 area, suggesting the clear seasonality with a large peak of activity in September.

Shallow earthquakes occur in the basin of the Mississippi (B6) located in the central United States. McGinnis (1963)[6] showed that the seismicity in this region

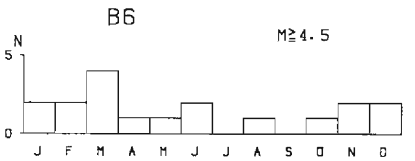

Fig. 13 Monthly distribution of earthquakes (M≧4.5) in the Mississippi area (B6).

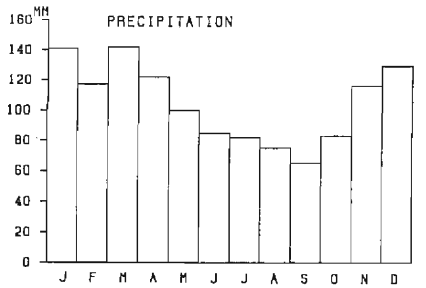

Fig. 14 Monthly mean precipitation at Memphis along the Mississippi river.

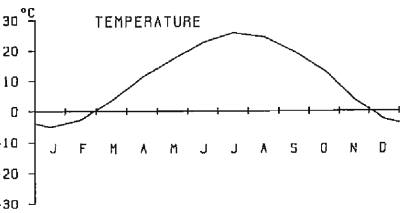

Fig. 15 Monthly mean temperature at Omaha in the upstream region of the Mississippi river.

varied corresponding to the water level of the Mississippi. **Fig. 13** shows the monthly distribution of earthquakes with magnitudes greater than or equal to 4.5. The data are not enough in number for our analysis, but **Fig. 13** shows that activity has a peak in March. Monthly precipitation at Memphis located along the Mississippi river has a peak in March as shown in **Fig. 14**. And the temperature at Omaha in the upstream region rises over the melting point in March, as shown in **Fig. 15**. All these phenomena suggest that the increase of the water in the Mississippi river may have a significant influence on the occurrence of earthquakes around this region.

4.3 Central America and Caribbean Sea region

The epicentral distributions of shallow earthquakes with magnitudes greater than or equal to 5.0 in Central America and the Caribbean Sea are shown in **Fig. 16** and **17**, respectively. These regions are divided into 13 areas (C1 to C5 and D1 to D8). Earthquakes in the northernmost area (C1) in Central America have a periodic pattern of distribution. **Fig. 18** shows monthly distribution of shallow earthquakes with magnitudes greater than or equal to 6.0 in the C1 area and the result of analysis. It shows the same pattern and peak as in the B1 area. On the other hand, no remarkable seasonal patterns are to be found in other areas. Four examples of the monthly distribution of shallow earthquakes are shown in **Fig. 19**. **Tables 3** and **4** are the results of the C2 and D6 areas, and they show that in both cases AIC become the minimum value when $J=4$ and $K=0$, indicating no seasonality.

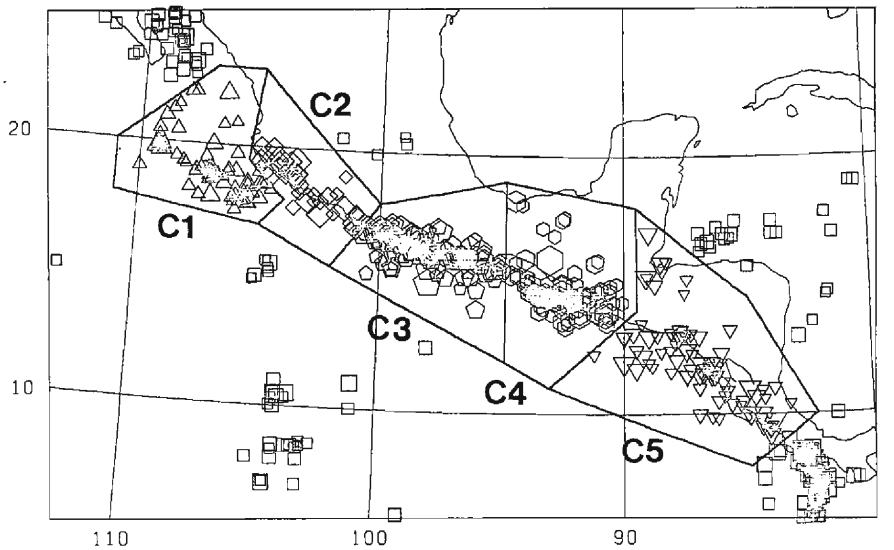

Fig. 16 Epicentral distribution of earthquakes ($M \geqq 5.0$) in the Central America region, and its division into 5 areas.

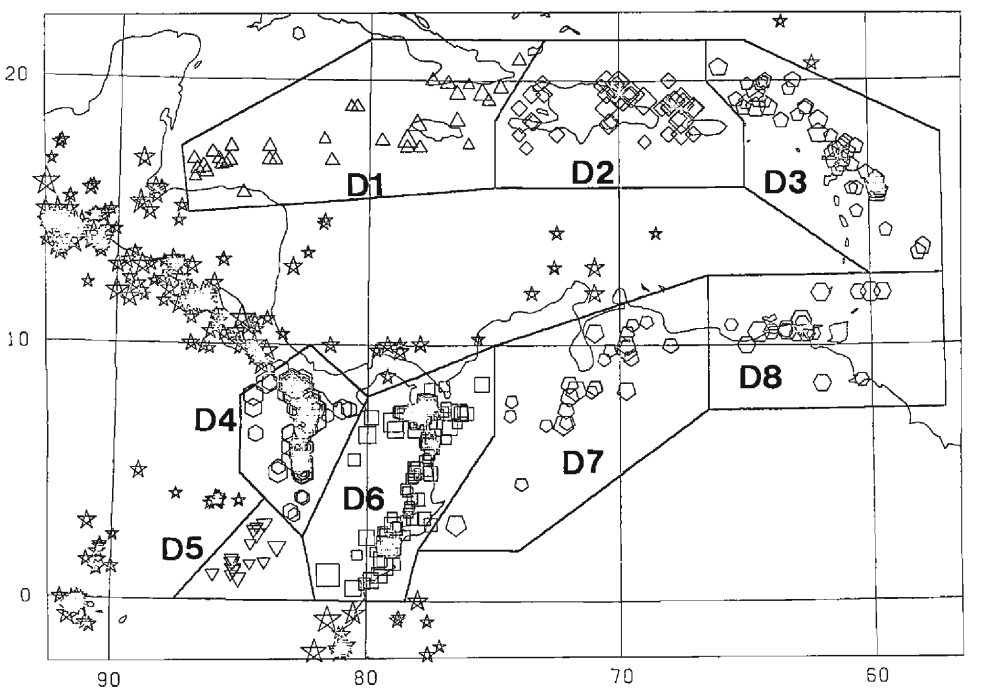

Fig. 17 Epicentral distribution of earthquakes ($M \geqq 5.0$) in the Caribbean Sea region, and its division into 8 areas.

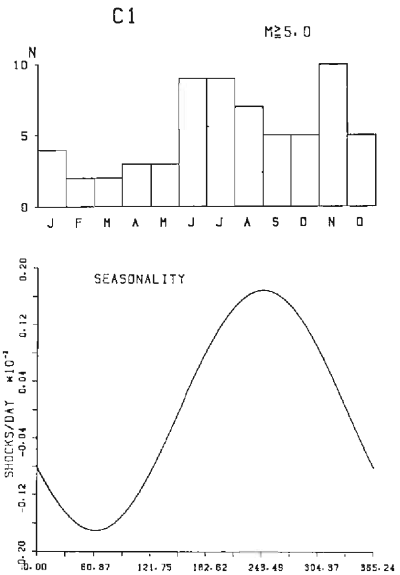

Fig. 18 Monthly distribution of earthquakes ($M \geqq 5.0$) and seasonal components calculated by the best fitting model in the northernmost area (C1) of Central America region.

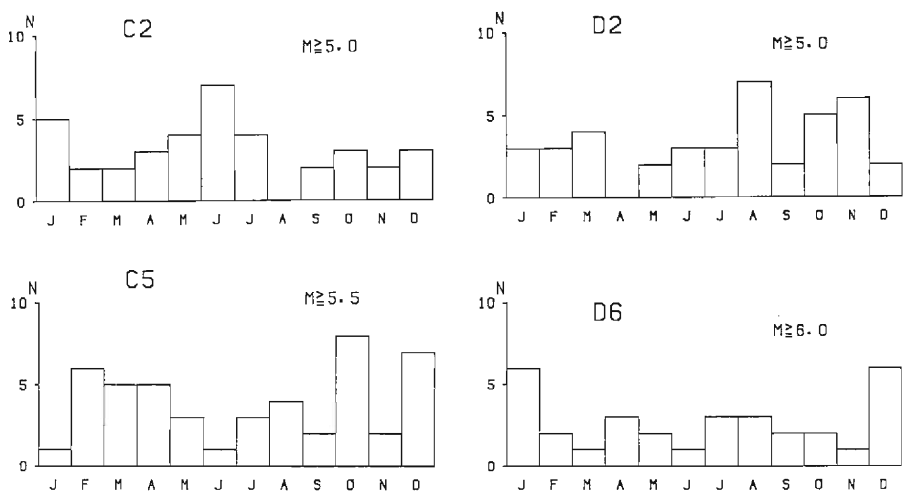

Fig. 19 Monthly distribution of earthquakes in the C2, C5, D2 and D6 areas.

Table 3 AIC of earthquakes in the C2 area. When the order of seasonal component K=0, AIC is minimum. It follows that there is no seasonality of seismic activities in the C2 area.

K \ J	0	1	2	3	4
0	557.90	554.51	556.26	557.52	549.22
1	560.30	556.52	558.15	559.27	553.19
2	562.32	557.98	559.93	561.52	557.09
3	564.34	560.98	562.76	564.12	560.65
4	566.52	564.18	566.09	567.71	563.86

Table 4 AIC of earthquakes in the D6 area. When J=4 and K=0, AIC is minimum. In this area, no seasonalities were found.

K \ J	0	1	2	3	4
0	566.88	560.64	561.81	563.13	560.62
1	569.47	561.81	563.28	565.11	564.40
2	572.22	563.78	565.54	567.08	567.19
3	574.77	566.63	568.37	570.25	569.71
4	574.47	568.94	569.94	571.08	571.32

4.4 South America region

Fig. 20 shows the epicentral distribution of shallow earthquakes in South America and the division into 8 areas (E1 to E8). Along the coastline many shallow earthquakes occur due to relative movements between the Nazca and South American plates under this area. The earthquakes in the crust are distributed inland from north to south. The monthly distribution of shallow earthquakes shows no particular features of seasonality as demonstrated by the four examples in **Fig. 21**.

Since the number of the inland earthquakes is not sufficient, we shall collect the earthquakes inside of an area bounded by the coastline and two latitudes of 0°N and 35°S into one group. **Fig. 22** shows the monthly distribution of this group, and slight increases are seen in summer and in winter. **Fig. 22** also shows the result on the same group. This pattern consists of annual and semi-annual components and it has two peaks in summer and in winter. **Table 5** shows AIC values, in which the minimum exists for J=0 and K=2. **Fig. 23** shows monthly mean precipitation in three cities of this region. The patterns are quite different between the coast and the mountains. Along the coast, precipitation throughout the year is very little in low latitude regions such as Lima. However, there is a peak around June in Sangiato in higher latitude regions. In mountain districts like La Paz there is a peak around January. One of the peaks of earthquakes in May or April corresponds to the time when the changing rate of precipitation in Santiago becomes maximum and another peak in November or December corresponds similarly to that in La Paz.

The shallow earthquakes of the oceanic group have no particular seasonalities, as shown in **Fig. 24**.

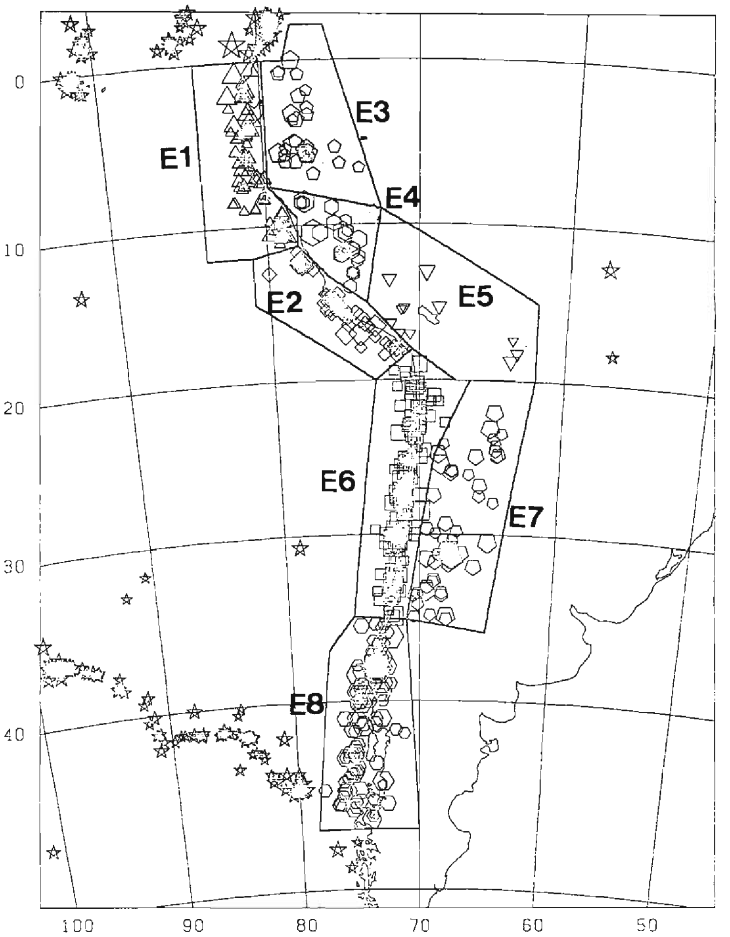

Fig. 20 Epicentral distribution of earthquakes ($M \geqq 5.0$) in the South America region, and its division into 8 areas.

Table 5 AIC of earthquakes in the land region of South America shown in Fig. 22.

K \ J	0	1	2	3	4
0	863.89	864.86	866.86	868.26	869.30
1	866.84	867.59	869.59	871.10	872.27
2	847.81	849.35	850.76	852.64	854.55
3	848.40	850.34	852.29	854.14	856.08
4	851.81	853.67	855.49	857.25	859.17

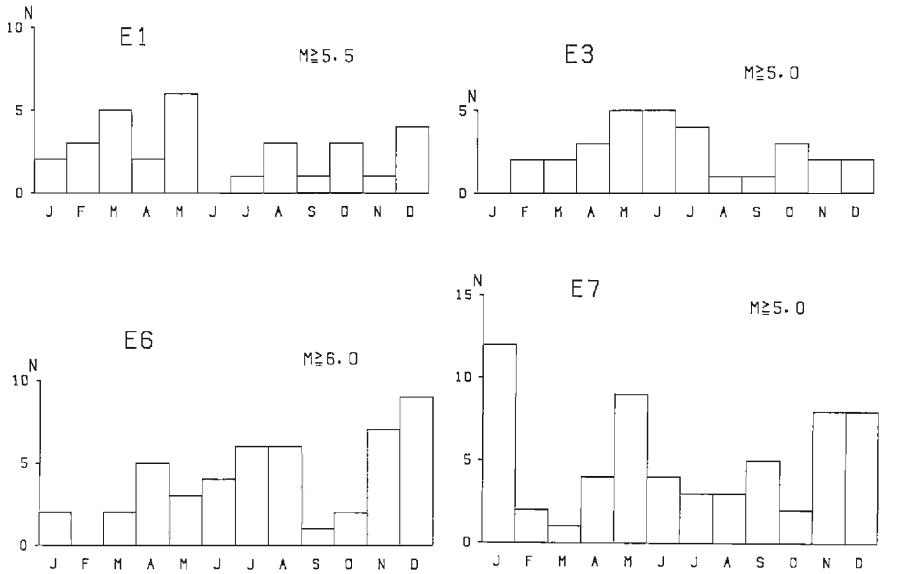

Fig. 21 Monthly distribution of earthquakes in the E1, E3, E6 and E7 areas.

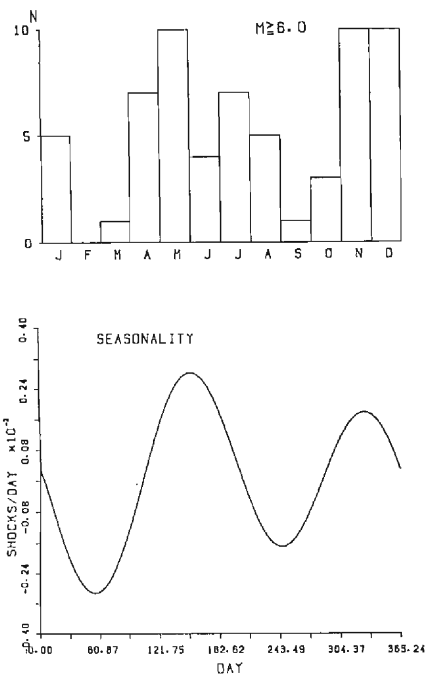

Fig. 22 Monthly distribution of earthquakes in the rearranged land region of South America from latitude 0°N to 35°S and seasonal components of the best fitting model.

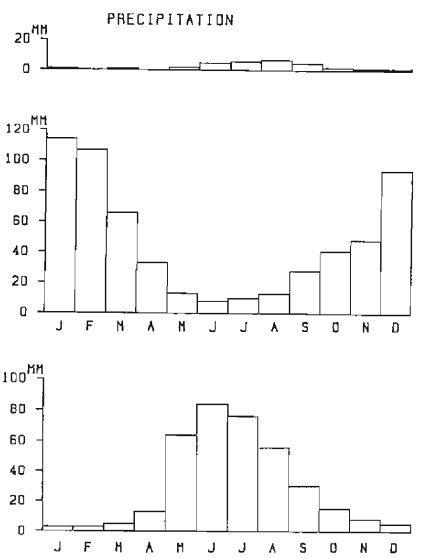

Fig. 23 Monthly mean precipitation in Lima (upper), La Paz (middle) and Santiago (lower).

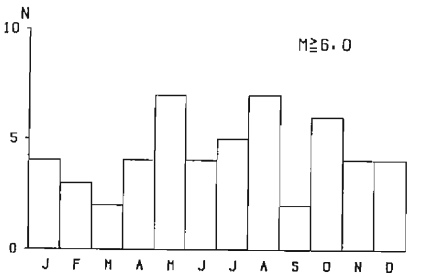

Fig. 24 Monthly distribution of earthquakes ($M \geqq 6.0$) in the oceanic region of South America.

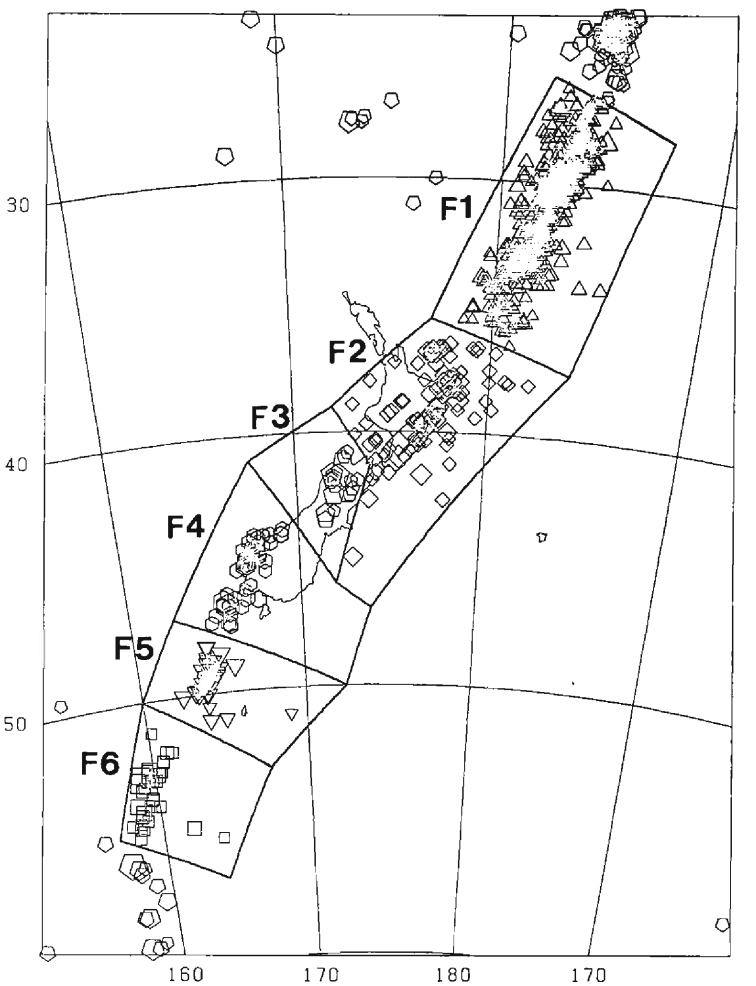

Fig. 25 Epicentral distribution of earthquakes ($M \geqq 5.0$) in and around New Zealand, and its division into 6 areas.

4.5 New Zealand region

The epicentral distribution of shallow earthquakes in and around New Zealand was divided into six areas (F1 to F6), as shown in **Fig. 25**.

Earthquakes that occurred in three areas off the coast of New Zealand (F1, F5 and F6) have no seasonalities as shown in **Fig. 26**. On the other hand, the monthly distributions in other three inland areas (F2, F3 and F4) show periodic patterns.

The F2 area includes North New Zealand and its surroundings. The pattern of monthly distribution of shallow earthquakes with magnitudes greater than or

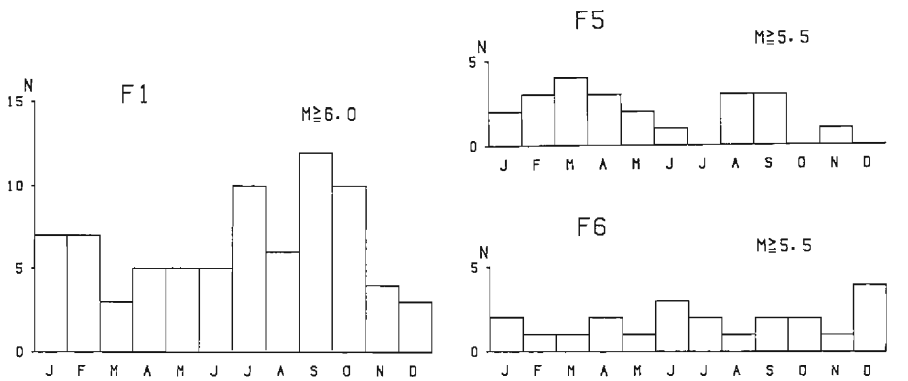

Fig. 26 Monthly distribution of earthquakes in the F1, F5 and F6 areas.

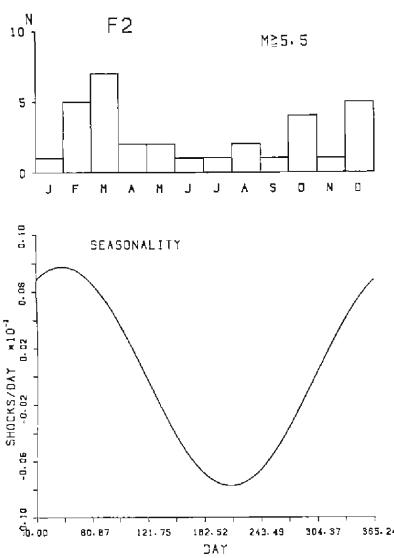

Fig. 27 Monthly distribution of earthquakes (M≧5.5) and seasonal components of the best fitting model in the F2 area.

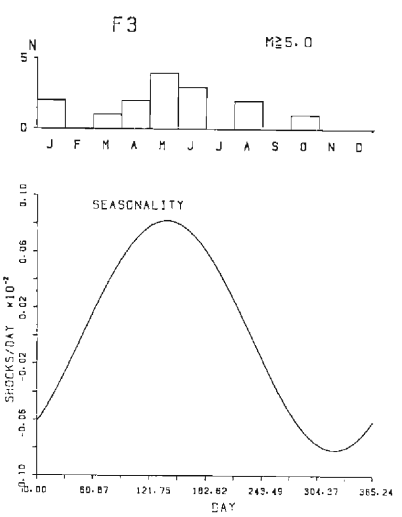

Fig. 28 Monthly distribution of earthquakes (M≧5.0) and seasonal components of the best fitting model of inland earthquakes in the north part of the South New Zealand (F3).

equal to 5.5 has a slight peak in summer as shown in **Fig. 27**. The result of analysis shows the existence of an annual variation with a peak in January as shown in the same figure.

In the F3 area, which is the north part of South New Zealand, almost all shallow earthquakes occur inland. The monthly distribution of shallow earthquakes with magnitudes greater than or equal to 5.0 and the result of analysis are both shown in **Fig. 28**. The annual component is predominant in this area as the same as in the F2 area, but the peak is a few months later than that in the F2 area.

The monthly distribution of shallow earthquakes with magnitudes greater than or equal to 5.5 in the F4 area, the south part of South New Zealand and its surroundings, appears to have three slight peaks as shown in the upper part of **Fig. 29**, but the result of analysis shows that a model with annual periodic component with a peak in June is best fitted to the data as shown in the lower part.

The data of monthly mean precipitation are available concerning four cities in New Zealand. Two of them are shown in **Fig. 30**. Monthly distributions of precipitation in Wellington and Christchurch show no large seasonal variations.

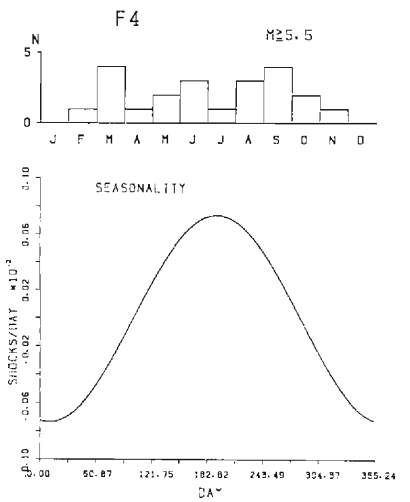

Fig. 29 Monthly distribution of earthquakes ($M \geqq 5.5$) and seasonal components of the best fitting model in the F4 area.

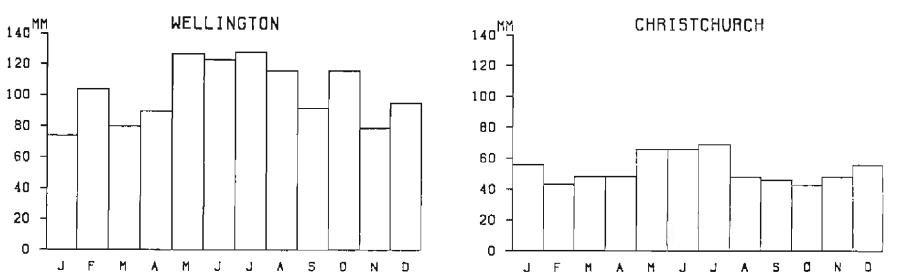

Fig. 30 Monthly mean precipitation at Wellington (left) and Christchurch (right).

But they have a peak around May to July and it corresponds to a peak of increasing rate of precipitation in May.

These results suggest that also in the land part of New Zealand the occurrence of shallow earthquakes appears to be related to rainfall.

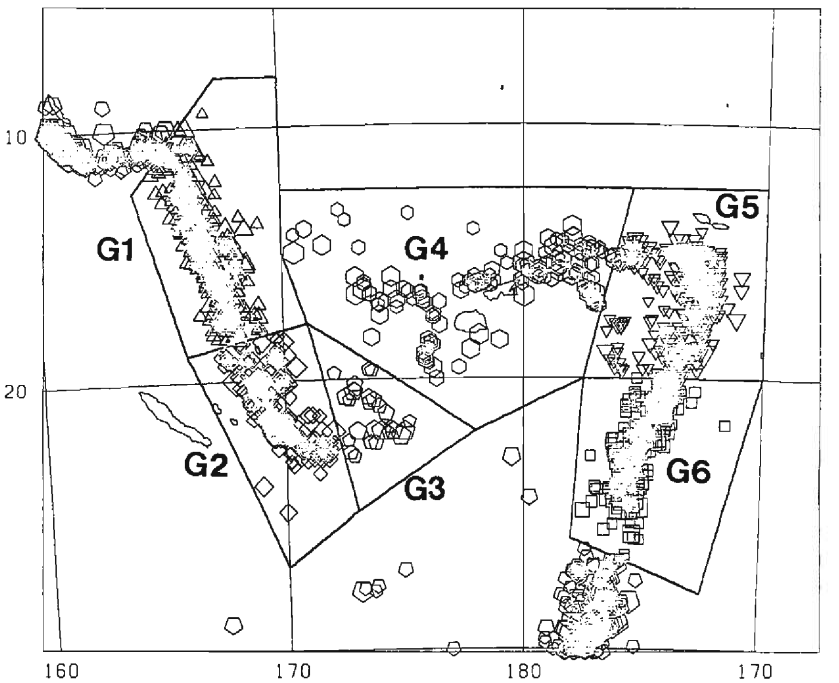

Fig. 31 Epicentral distribution of earthquakes ($M \geqq 5.0$) in and around Fiji of the Southwest Pacific Ocean region, and its division into 6 areas.

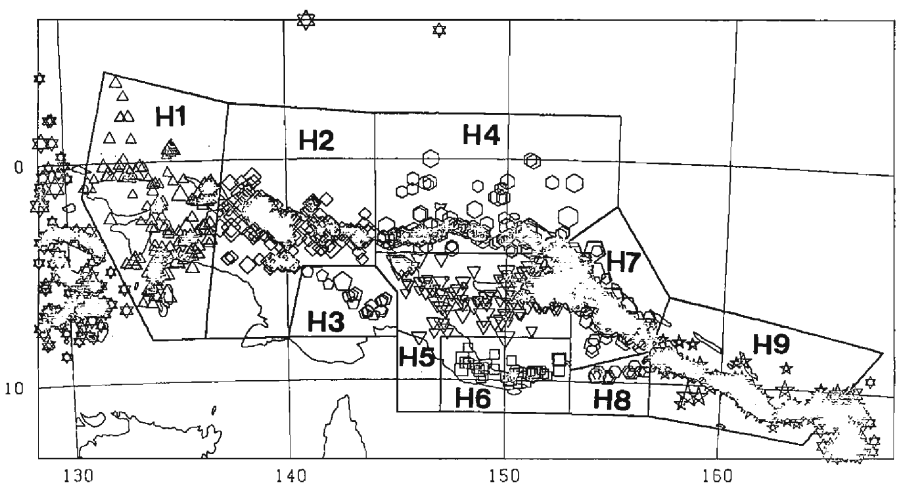

Fig. 32 Epicentral distribution of earthquakes ($M \geqq 5.0$) in and around New Guinea of the Southwest Pacific Ocean region, and its division into 9 areas.

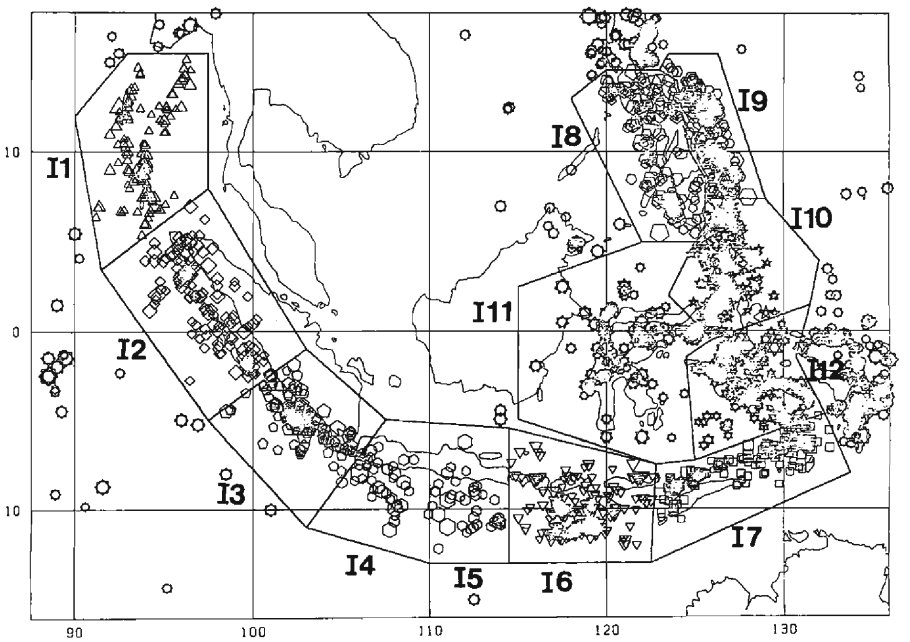

Fig. 33 Epicentral distribution of earthquakes (M≧5.0) in and around Indonesia of the Southwest Pacific Ocean region, and its division into 12 areas.

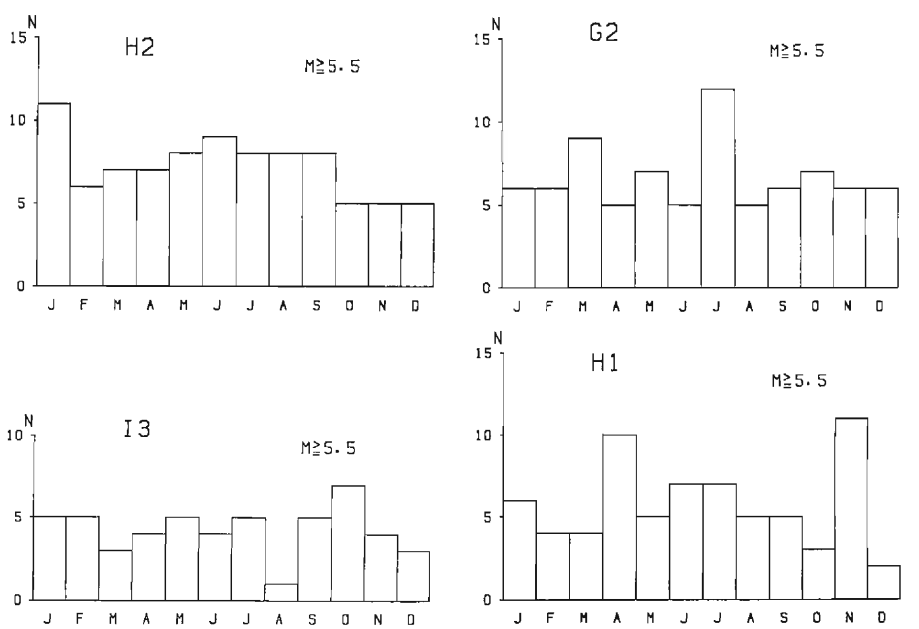

Fig. 34 Examples of monthly distribution of earthquakes in the Southwest Pacific Ocean.

4.6 Southwest Pacific Ocean region

This region is divided into 26 areas (G1 to G6, H1 to H9 and I1 to I11), considering spatial distributions of earthquakes. **Fig. 31**, **32** and **33** show the epicentral distributions of shallow earthquakes and its division of the region. The results indicate that the seismic activity in each part has no seasonal variations. The monthly distributions of shallow earthquakes with magnitudes greater than or equal to 6.0 have no particular peaks as shown by examples in **Fig. 34**. In this region almost all earthquakes occur in the ocean area.

4.7 Japan Island region

The epicentral distribution of shallow earthquakes with magnitudes greater than or equal to 5.0 in the Japan Island region is shown in **Fig. 35**. This region

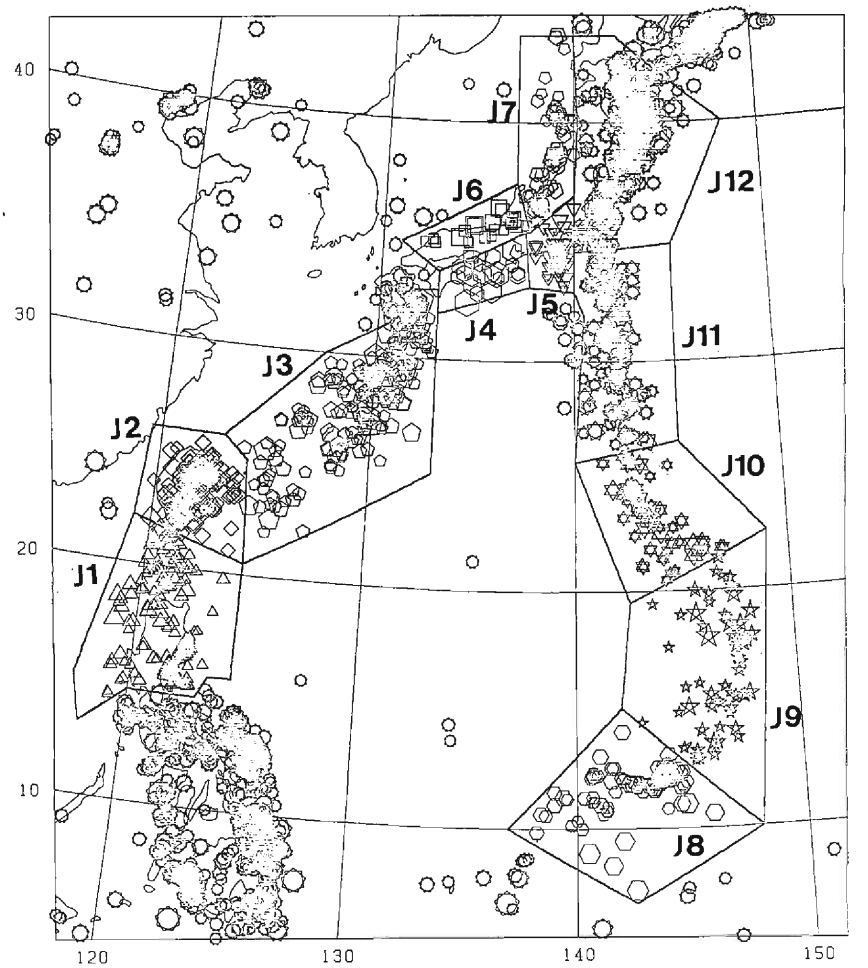

Fig. 35 Epicentral distribution of earthquakes ($M \geqq 5.0$) in the Japan region, and its division into 12 areas.

is divided into 12 areas (J1 to J12). **Fig. 36** shows monthly distribution of earthquakes in some areas. Seismic activities of almost all areas have no seasonalities. Only in the Inner and Outer Zone of Southwest Japan (J4 and J6) are the seasonal variations of seismic activities found.

The periodic pattern calculated from the point process model in the Outer Zone of Southwest Japan (J4) is shown in **Fig. 37**. The peak of seismic activity is in winter, and this result coincides with that by Mogi (1969)[4] in the case of larger earthquakes. More detailed analysis and discussion on this area will be given in a later chapter.

In Northeast Japan no seasonal variations of activity were found as far as shallow earthquakes with magnitudes greater than or equal to 5.0 are concerned, though

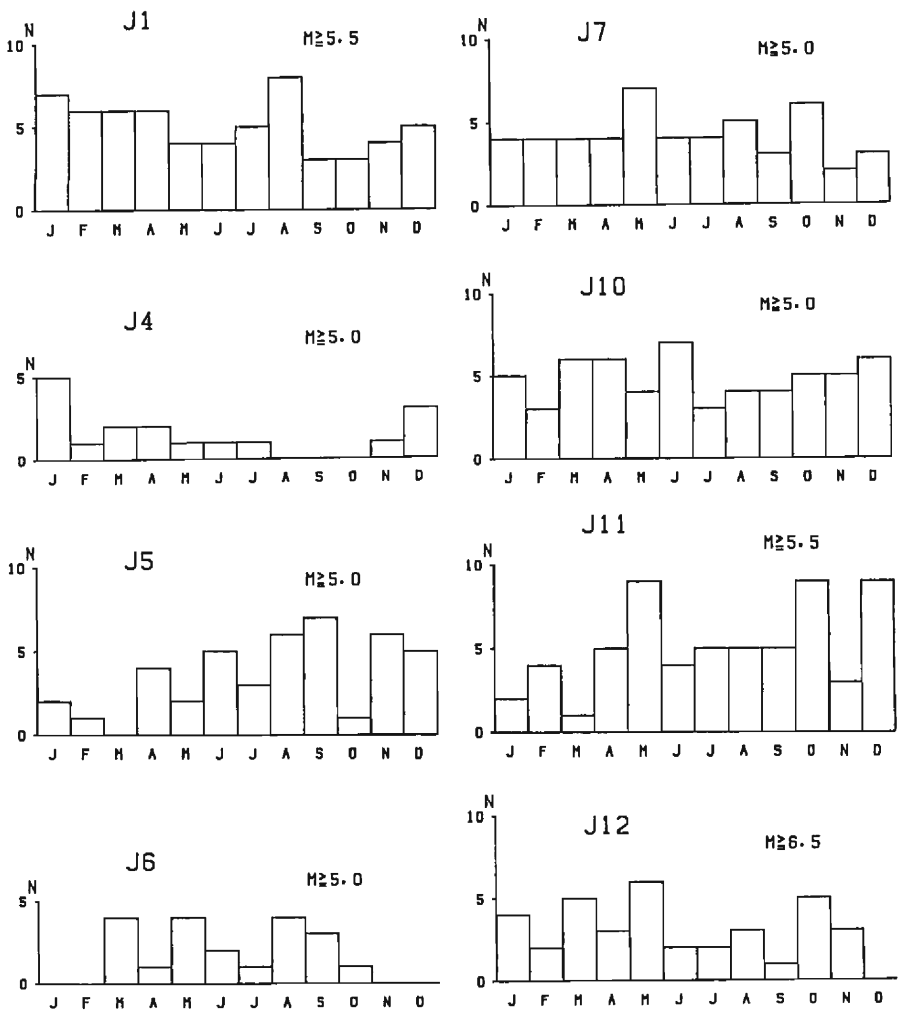

Fig. 36 Examples of monthly distribution of earthquakes in the Japan region.

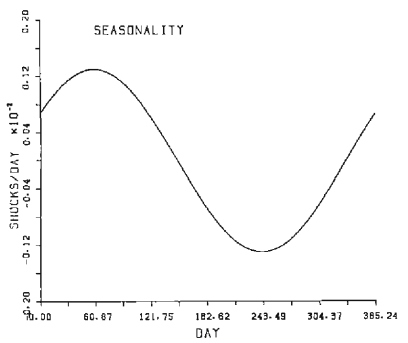

Fig. 37 Seasonal component calculated by the best fitting model in the Outer Zone of Southwest Japan (J4).

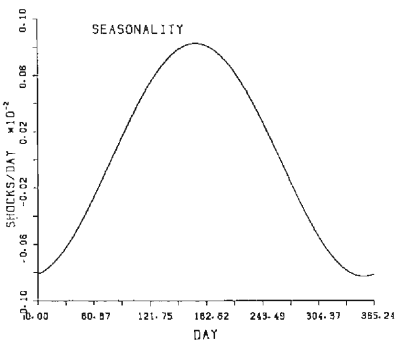

Fig. 38 Seasonal component calculated by the best fitting model in the Inner Zone of Southwest Japan (J6).

the result by Mogi (1969)[4] indicated seasonality for larger earthquakes ($M \geqq 7.5$) in this area.

The result of analysis on the activity in the Inner Zone shows that there exists seasonal variation as shown in **Fig. 38**, which coincides with the results by Oike (1977)[5] and Ogata (1983)[17]. Detailed analyses and discussions on this area will be given in the following chapter.

4.8 Kuril and the western Aleutian Islands region

This region was divided into 5 areas (K1 to K5) as shown in **Fig. 39**. In 4 areas along the trench (K2 to K5), activity of interplate earthquakes is high caused

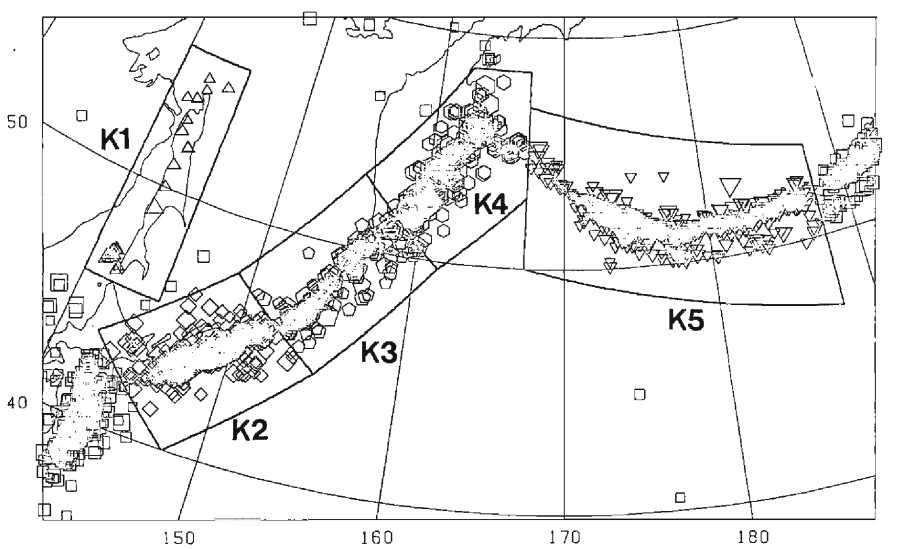

Fig. 39 Epicentral distribution of earthquakes ($M \geqq 5.0$) in the Kuril and western Aleutian region, and its division into 5 areas.

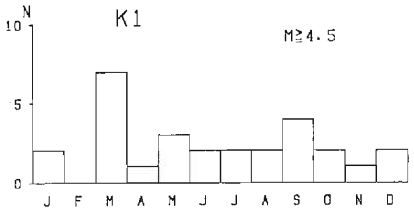

Fig. 40 Monthly distribution of earthquakes (M≧4.5) in Sakhalin (K1).

by relative movements between the Pacific and Eurasian plates. However, their activity has no seasonality. **Fig. 40** shows the monthly distribution of the inland shallow earthquake in Sakhalin (K1), and no seasonality was found in this area, either.

4.9 The central and western part of China and Himalayan region

This region is divided into 4 areas (L1 to L4 in **Fig. 41**). The size of each area is larger than those of other regions so far treated. A lot of earthquakes occur along the Himalayans due to the relative movements between the Indian and Eurasian plates. No seasonal characteristics were found in these areas (L2 to L4).

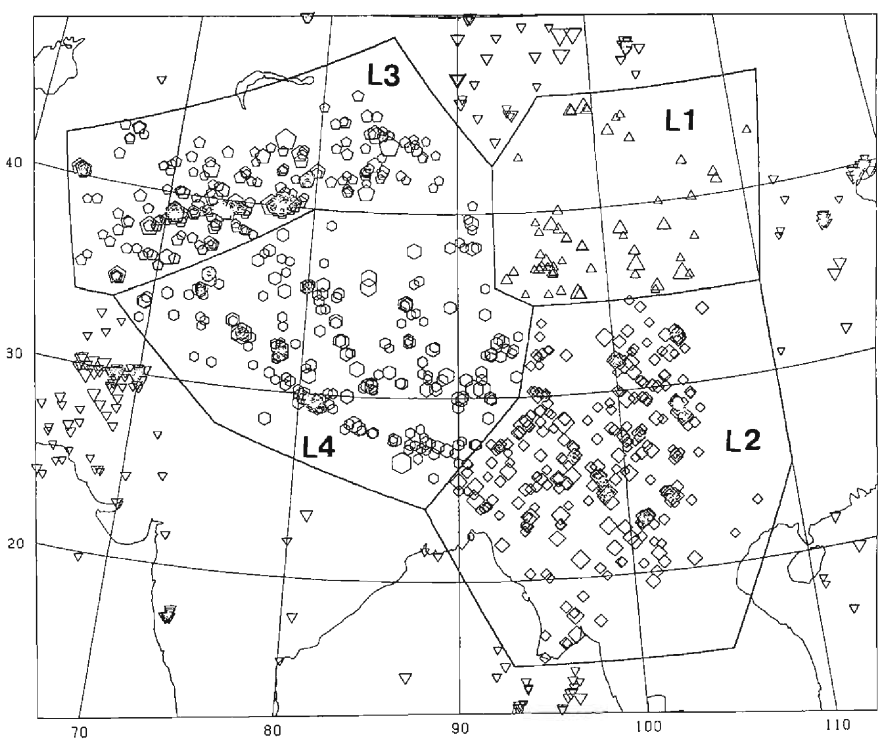

Fig. 41 Epicentral distribution of earthquakes (M≧5.0) in the central and western part of China and Himalayan region, and its division into 4 areas.

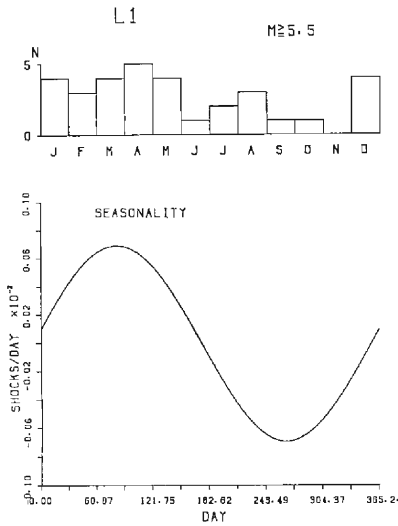

Fig. 42 Monthly distribution of earthquakes ($M \geqq 5.5$) and seasonal component calculated by the best fitting model in the central part of China (L1).

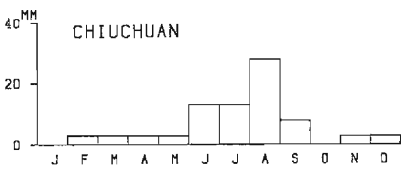

Fig. 43 Monthly mean precipitation at Chiuchuan in the central part of the L1 area.

Only in the central part of China (L1), where there is a wide distribution of shallow earthquakes, is the seasonal variation of activity found. **Fig. 42** shows the monthly distribution of shallow earthquakes with magnitudes greater than or equal to 5.5, and the periodic pattern calculated by the point process analysis. This area consists mainly of desert, so precipitation is generally very little. **Fig. 43** shows the monthly distribution of precipitation at Chiuchuan, which is located in the center of L1 area. Although it has a peak around August, it is difficult to discuss any relation between seasonal variation of earthquakes and meteorological phenomena in this area because of too small amount of precipitation. A part of these earthquakes occurs along a long river which carries plenty of water from the Tsinghai plateau far from this area. For example, along the Yellow River, floods were brought about in summer by heavy rainfall in the Tsinghai area. More detailed data of meteorology and the river are necessary for any detailed analysis and discussion of this area.

As epicentral data from the northeastern part of China are insufficiently recorded in NOAA's file, the seismic activity there will be examined in detail in the next chapter by using other kind of long-term historical earthquake data.

Seismic activity in Korea is also examined in the next chapter, using an available historical earthquake data set.

4.10 The Middle East region

Epicentral distribution of shallow earthquakes in the Middle East region with magnitudes greater than or equal to 5.0 is shown in **Fig. 44**. This region is divided

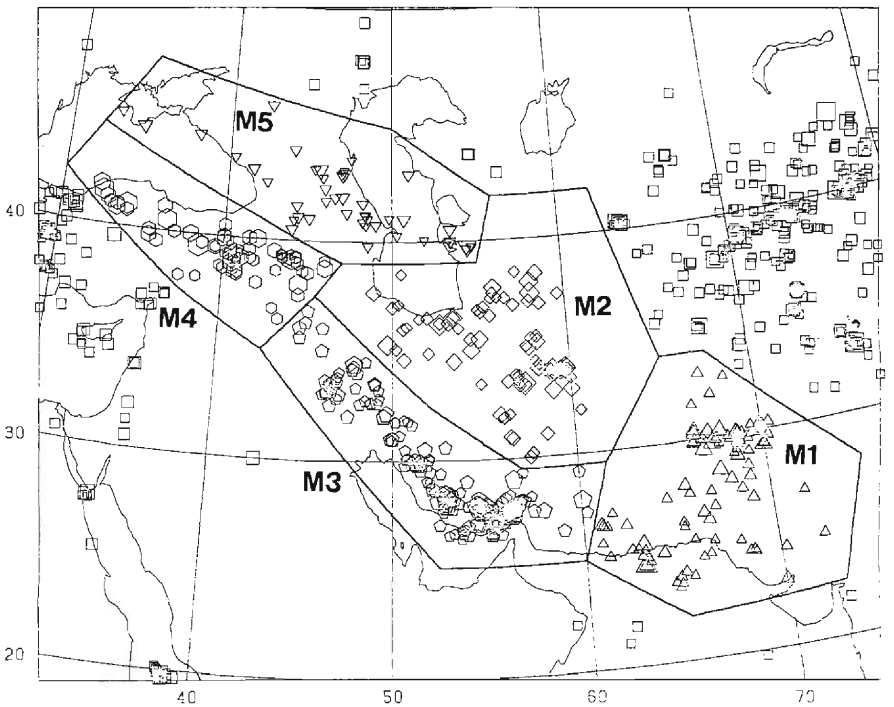

Fig. 44 Epicentral distribution of earthquakes ($M \geqq 5.0$) in the Middle East region, and its division into 5 areas.

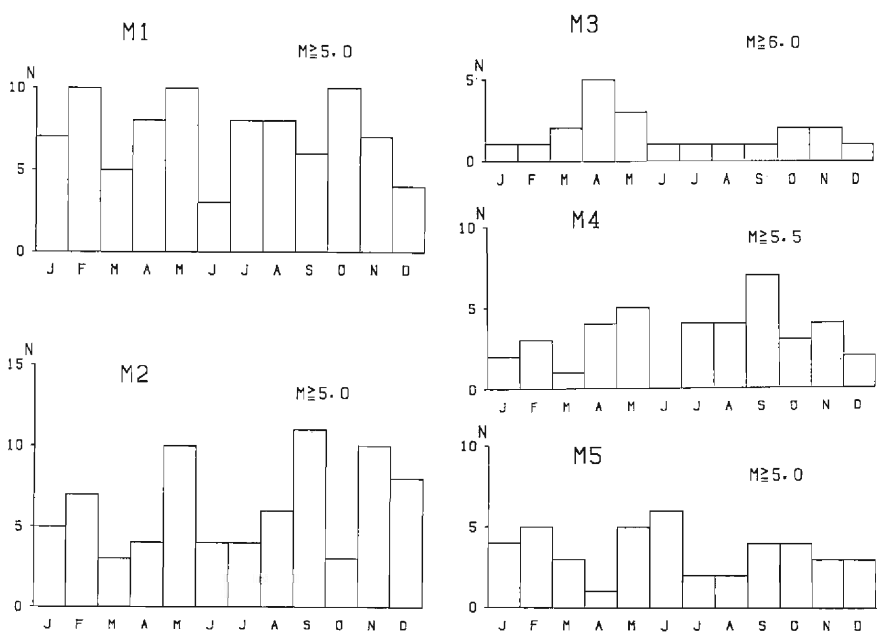

Fig. 45 Monthly distribution of earthquakes in each area of the Middle East region.

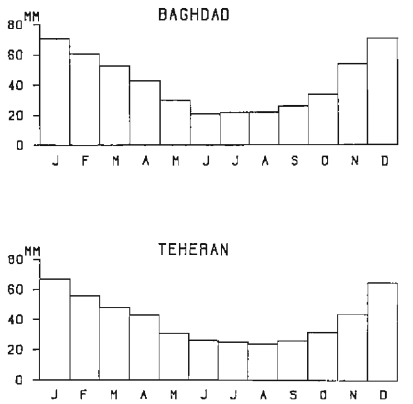

Fig. 46 Typical monthly distributions of precipitation in the Middle East region. The upper and lower correspond to Baghdad and Teheran, respectively.

into 5 areas (M1 to M5). The monthly distribution of earthquakes shows no peculiar pattern in any area, as shown in **Fig. 45**. **Fig. 46** shows two typical monthly distributions of precipitation in this region. In this region, the level of precipitation is not always low, but its changing rate is very low.

4-11. The Mediterranean Sea region.

The epicentral distribution of shallow earthquakes with magnitudes greater than or equal to 5.0 in the Mediterranean Sea region and division of this region into 7 areas (N1 to N7) are shown in **Fig. 47**.

Seasonal variations have been detected in two areas (N2 and N3) around the Aegean Sea. The monthly distribution of earthquakes with magnitudes greater

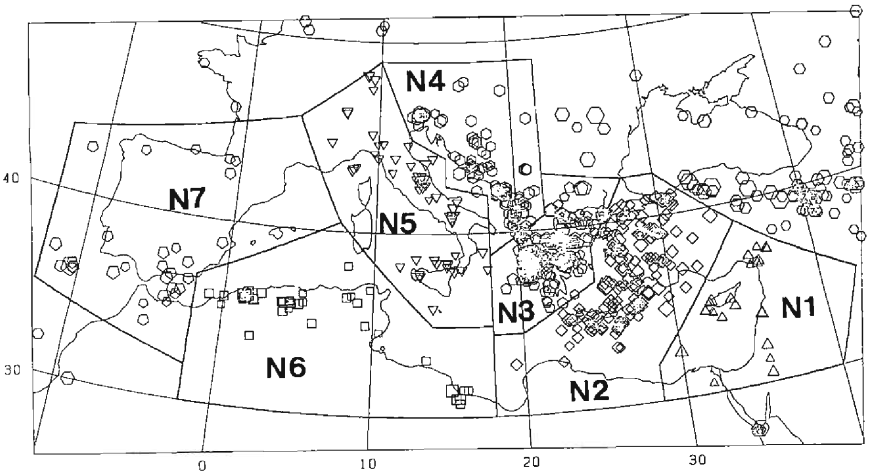

Fig. 47 Epicentral distribution of earthquakes ($M \geqq 5.0$) in the Mediterranean Sea region, and its division into 6 areas.

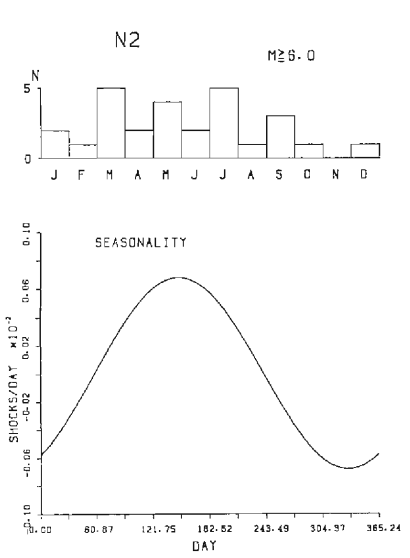

Fig. 48 Monthly distribution of earthquakes (M≧6.0) and seasonal component calculated by the best fitting model in the N2 area.

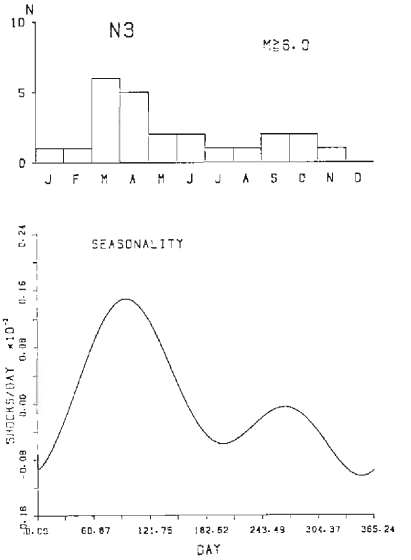

Fig. 49 Monthly distribution of earthquakes (M≧6.0) and seasonal component calculated by the best fitting model in the N3 area.

than or equal to 6.0 and its periodic pattern in the N2 and N3 areas are shown in **Fig. 48** and **Fig. 49**, respectively. In the Turkey area (N2), monthly distribution of earthquakes is not so concentrated in a certain month, but a model with an annual periodic component fits best to the data, as shown in **Fig. 48**.

In the Greece area (N3), earthquakes occur concentratively in March. The best fitting model has two periodic components, annual and semi-annual. There are two peaks, a larger one in March and a smaller one in October. As almost all earthquakes in this area occur off shore, seismic activity can not be affected by such meteorological phenomena as precipitation.

No seasonal variations were detected in the N5 area which includes Italy and its surroundings as shown in **Fig. 47**. This may be explained by the fact that this area (N5), consists of various districts with very different climates. Therefore, we shall adopt only the land part of the Italian Peninsula, as shown in **Fig. 50**. **Fig. 51** shows the monthly distribution of shallow earthquakes with magnitudes greater than or equal to 5.0 in this area. The periodic pattern of the best fitted point process model is also shown in **Fig. 51**. The model has an annual component and its pattern resembles the distribution of monthly mean precipitation in Rome (**Fig. 52**). The peak of seismicity coincides with the peak of the increasing rate of precipitation, as compared in **Fig. 52**.

5. Detailed discussion on the East Asian region

In China there are a lot of historical documents or data on earthquakes. Epicentral data files have been compiled by analyzing those documents. The nature

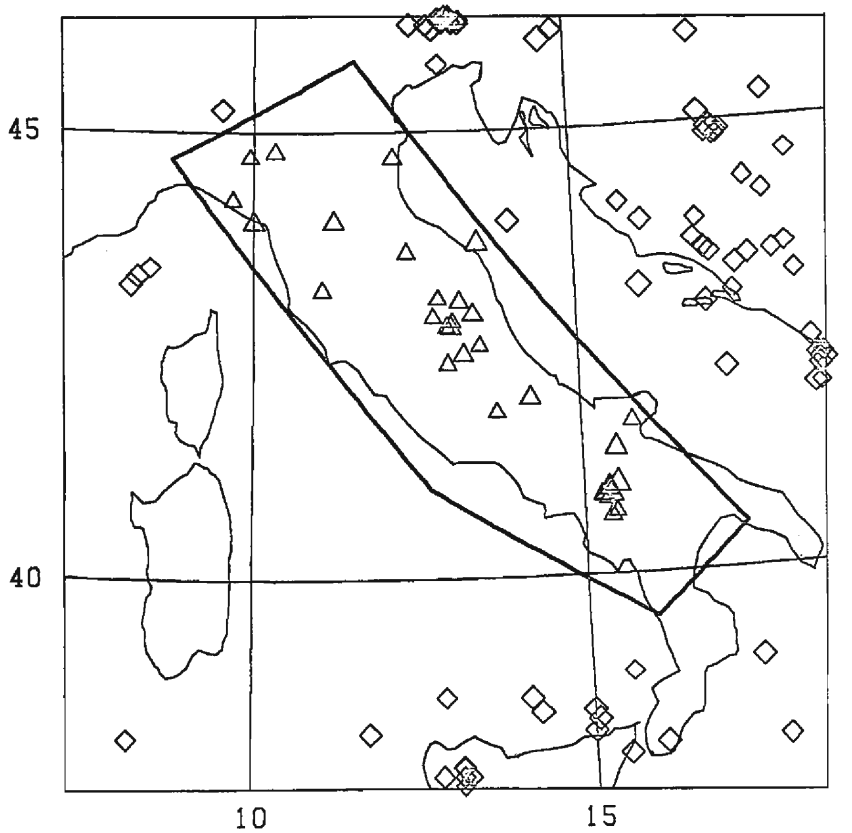

Fig. 50 Epicentral distribution of earthquakes ($M \geqq 5.0$) in the inland part of Italy.

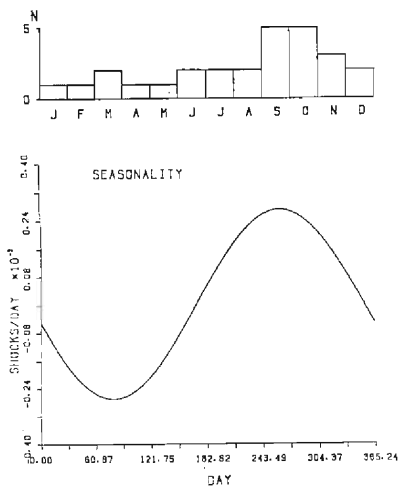

Fig. 51 Monthly distribution of earthquakes ($M \geqq 5.5$) and seasonal components of the best fitting model in the inland part of Italy.

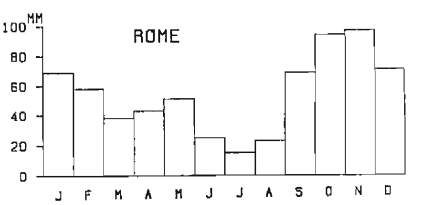

Fig. 52 Monthly distribution of precipitation in Rome.

of seismic activity has been investigated on the basis of those data by Oike et al (1982)[22], Oike (1984)[23] and Matsumura et al (1985)[24].

Fig. 53 shows the distribution of large shallow earthquakes with magnitudes larger than or equal to 7.5 in East Asia. The large active faults, trenches and troughs are shown in the figure by solid lines. It is noticed that almost all great earthquakes occur along those tectonic lines. The west part of china has few historical documents and so some great earthquakes in this area might have been missed. No great earthquakes occurred in the southeast of China. It is clear by analyses of recent earthquake data that seismicity in this area is very low.

The monthly distribution of great earthquakes in each province of China was examined from historical earthquake data. In such cases where historical earthquake data are used for statistical analyses, a problem always arose as to the accuracy of data. Small earthquakes might have been missed because of little damage, and even great earthquakes might not have been recorded due to occurrence in low population areas. The data used in this paper may have much irregularity in accuracy, according to the time and place. However, as the irregularity of data is in a cycle of several tens of years or more, the monthly distribution of great earthquakes will not be affected by such irregularity.

In this paper, greater earthquakes in the eastern part of China under good detection capability were analyzed, and western China, where historical earthquake data are few, is not discussed. **Fig. 54** shows the distribution of large cities in China and Korea for understanding their respective situations.

The monthly distributions of earthquakes with magnitudes greater than or

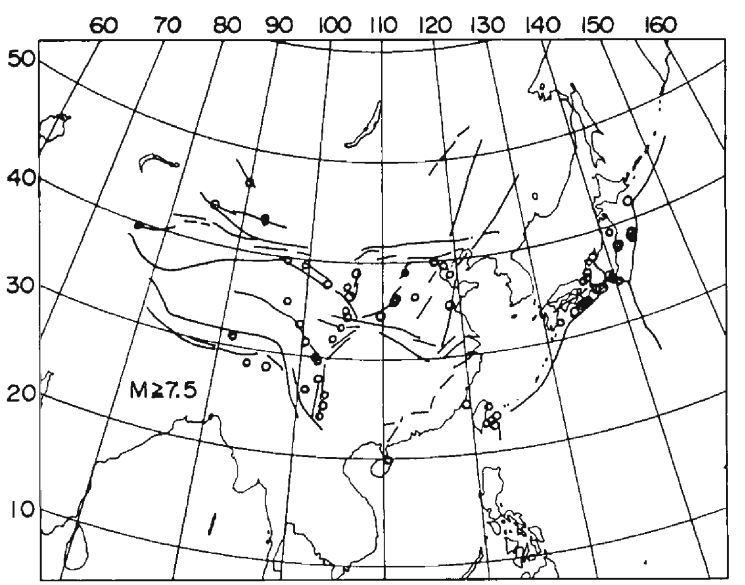

Fig. 53 Distribution of large shallow earthquakes (M≧7.5) and active tectonic lines in East Asia.

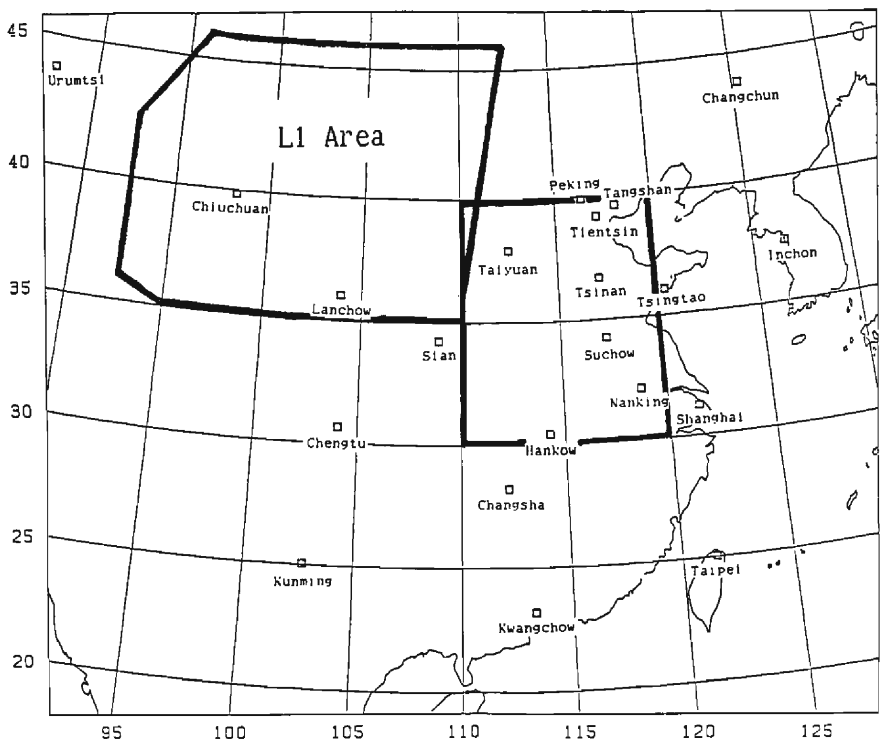

Fig. 54 Map of China and Korea.

equal to 6.0 are also shown in **Fig. 55** together with precipitation for some provinces where great earthquakes occurred frequently. Patterns of the monthly mean precipitations appear simple and similar in all areas. The peak of precipitation corresponds to the period from June to July. In the northeastern provinces, Hopei, Shansi and Shantung, great earthquakes have occurred concentratively in a certain season.

In the southern region where the level of seismicity is very high, many great historical earthquakes have occurred. The monthly distribution of earthquakes in this region has no special features and has no relation to the monthly mean precipitation. In Kwantung Province there were few historical earthquakes. Even with the recent observations of earthquakes, low seismicity is found there.

Since patterns of monthly mean precipitation mutually resemble each other so much in the eastern provinces of China, the total monthly distribution of historical great earthquakes in these provinces has been examined. **Fig. 56** shows the monthly distribution of earthquakes with magnitudes greater than or equal to 7 in the provinces except the Taiwan province and the western regions (the Sinkiang Uighur and Tibetan automous regions and the Tsinghai province). More than one third of the earthquakes with magnitudes greater than or equal to 7.0 in this region have occurred in the season from May to July. As for great earthquakes

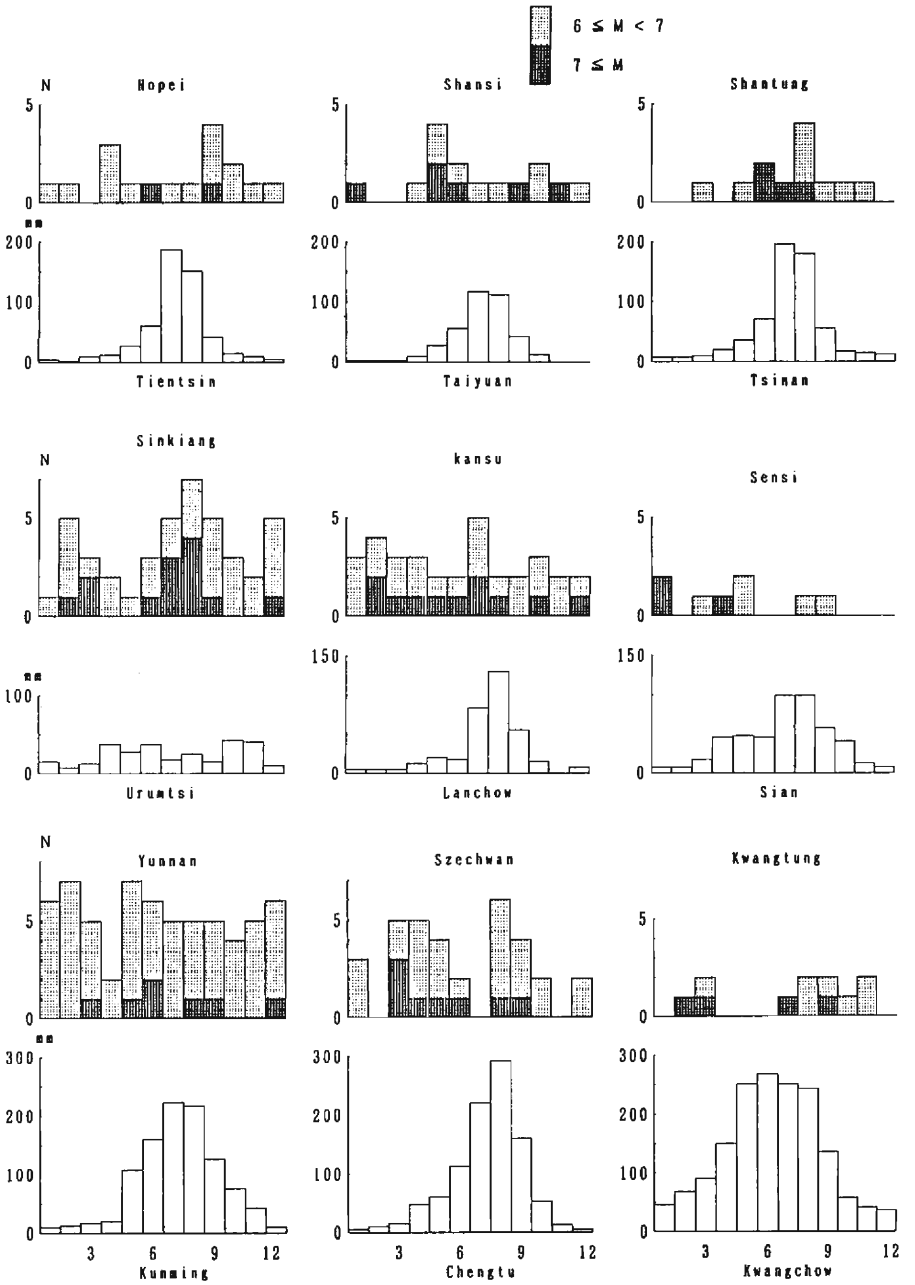

Fig. 55 Monthly distribution of earthquakes (M≧6.0) of provinces where great earthquakes occurred frequently in China and monthly mean precipitation of the largest city in each province.

Fig. 56 Monthly distribution of earthquakes ($M \geqq 7.0$) in the eastern province except the Taiwan province.

with magnitudes greater than or equal to 7.5, more than a half of them have also occurred in that season. This pattern of distribution is quite similar to that of monthly mean precipitation or its increasing rate. The peak distribution of earthquakes corresponds to the transition from dry to wet season.

The more limited area of the northeastern part of China was adopted in order to examine the relation between earthquake occurrence and precipitation. **Fig. 57** shows the monthly distribution of great earthquakes with magnitudes of 7.0 or more in a rectangular area from 110°E to 120°E and from 30°N to 40°N. The lower part of **Fig. 57** shows the monthly mean precipitation at Tsinan, which is the typical case in this area. 7 great earthquakes with magnitudes of 7.5 or more occurred in this area and all of them occurred from May to September. As there are so many long-term historical documents in this area, earthquake data are more accurate than in other areas and so we can examine even smaller earthquakes. Earthquakes

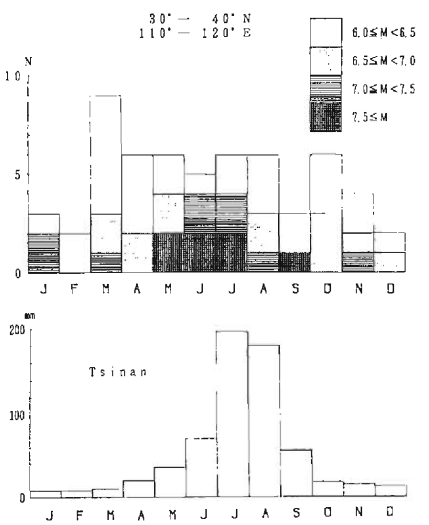

Fig. 57 Monthly distribution of earthquakes ($M \geqq 7.0$) in the rectangular area from 110°E to 120°E and from 30°N to 40°N, and the monthly mean precipitation in Tsinan.

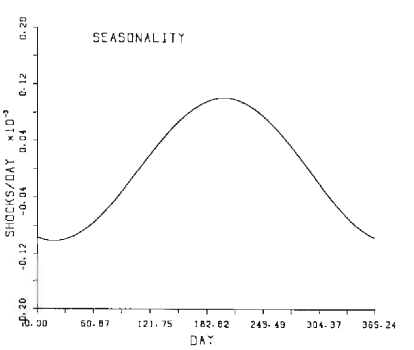

Fig. 58 Seasonal components of the best fitting model of historical earthquakes ($M \geqq 7.0$) in the rectangular area from 110°E to 120°E and from 30°N to 40°N.

with magnitudes greater than or equal to 6.5 tend to occur concentratively.

The seasonal variation of occurrence of earthquakes with magnitudes greater than or equal to 7.0 in this area analyzed by the point process model is shown in **Fig. 58**. The periodic component is annual and its peak corresponds to June or July. This coincides with the nature of the monthly distribution of precipitation or its rate of change in this region.

Fig. 59 shows daily precipitation from February to September, 1976 in Tangshan city. The great Tangshan earthquake of M 7.8 occurred on July 28, 1976. The daily precipitation just before the main shock shows that this earthquake might have been triggered by remarkable heavy rainfall in the epicentral region. **Fig. 60** shows spatial distribution of precipitation from July 25 to July 27 in this region. Heavy rainfall was concentrated around the main shock and the largest aftershock which is shown by crosses in the figure.

Kim and Suh (1977)[20] compiled historical earthquake data in Korea by analyzing various historical documents. This data set contains 443 earthquakes since A.D. 27 to 1977. The magnitudes of earthquakes in this set are not determined and only the intensities in JMA scales were reported. The maximum intensity

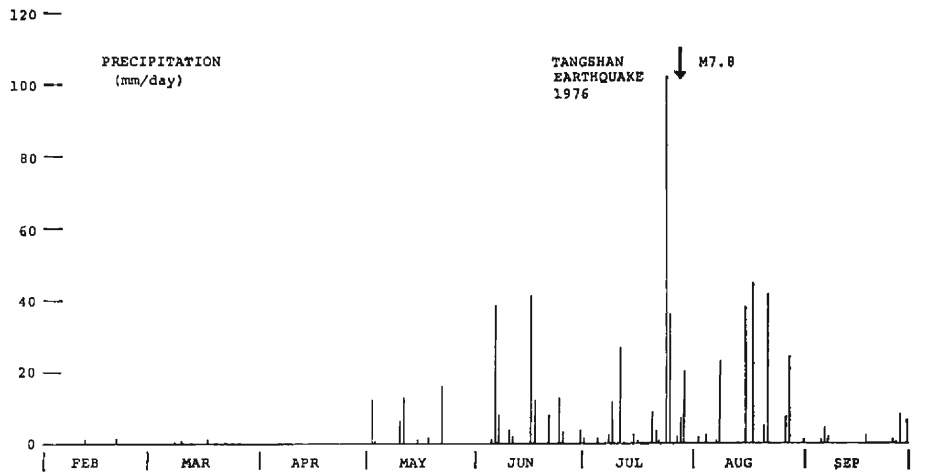

Fig. 59 Daily precipitation in the epicentral region of the great Tangshan Earthquake.

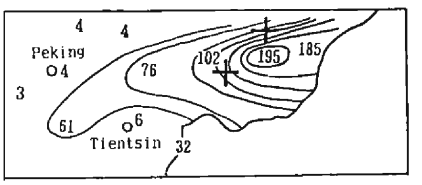

Fig. 60 Distribution of precipitation from July 25 to 27 just before the great Tangshan Earthquake. Two crosses indicated epicenters of the main shock and the greatest aftershock.

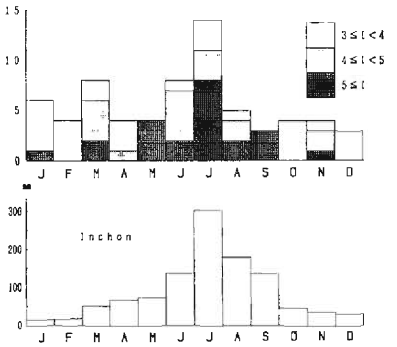

Fig. 61 Monthly distribution of earthquakes in Korea and monthly mean precipitation at Inchon along the west coast of the Korean Peninsula.

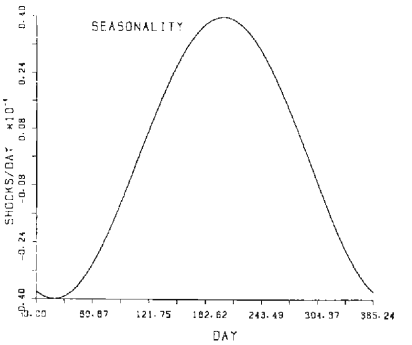

Fig. 62 Seasonal components of the best fitting model of earthquakes with JMA intensity 5 in Korea.

included in the data set is 5. This means that seismicity in Korea is not high compared with neighboring regions. Because of the lack of smaller earthquakes before the 17th century in the historical documents, earthquakes with intensities less than 5 were omitted in the present analysis.

In the 18th century, no earthquakes were reported in this data set. This does not mean the lack of documents but really few big events near the Korean peninsula (Oike et al, 1982)[22]. In **Fig. 61**, showing monthly distribution of earthquakes in Korea, the peak of this distribution is in July. The lower part of **Fig. 61** shows the monthly distribution of mean precipitation in Inchon. In all other prefectures of Korea, the patterns of monthly precipitation are similar to that at Inchon. The pattern of periodic components, as shown in **Fig. 62**, consist of only annual component with its peak in July. This peak distribution of earthquake activity coincides with that of precipitation. This result suggests that there appears is a close relation between rainfall and earthquake occurrence in Korea.

6. Detailed discussions on Southwest Japan

6.1 The Inner Zone of Southwest Japan

Ogata (1983)[17] analyzed the temporal distribution of earthquakes in the Inner Zone of Southwest Japan, applying the point process model and using the data from the Seismological Bulletin of JMA from 1965 to 1980. Seasonal components of the minimum AIC model that is obtained considering the clustering effect by aftershocks consists of three periodicities, annual, semi-annual and every third of a year. Smoothed precipitation curve has similar variations to the seasonal component.

His results are referred to in **Fig. 63**. The biggest peak of seismic activity is found in September and minor peaks in June and March. These correspond to peaks of the increasing rate of precipitation.

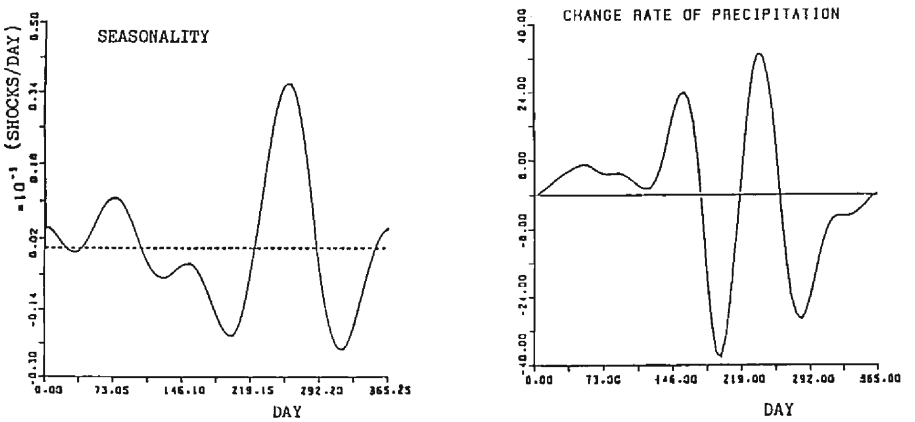

Fig. 63 Result from JMA data in the Inner Zone of Southwest Japan referred from Ogata (1983). The left and right correspond to seasonal component of the best fitting model and the change rate of precipitation, respectively.

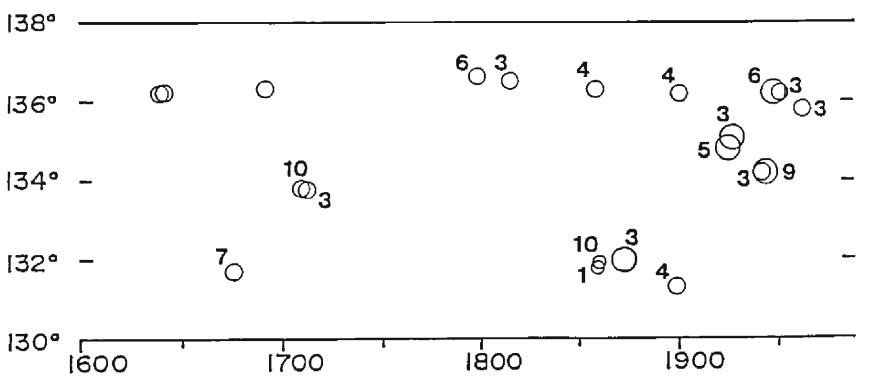

Fig. 64 Space-time plots of large earthquakes in the Inner Zone of Southwest Japan. Numbers indicate the month of occurrence of shocks.

Fig. 64 shows a space and time plot of earthquakes in the Inner Zone from the historical data. The number in each circle shows the month of the occurrence. From this figure it is recognized that in this region one large event is followed by other shocks in the neighboring area, and also that they occur in the season corresponding to the peaks indicated in **Fig. 63**.

Microearthquakes in this region have been observed by the Tottori Microearthquake Observatory of Disaster Prevention Research Institute, Kyoto University since June, 1965 and hypocentral data have been compiled by Oike (1975)[25]. There are many active faults in this region and many microearthquakes occur along them. Oike (1977) showed that small swarm type activities along the Yamasaki fault were clearly related to sudden changes of strain across the fractured zone by a heavy rainfall. Namely, he mentioned that in several days after a heavy rainfall large relative movements of bed rocks between the fractured zone were observed and then microearthquakes occurred.

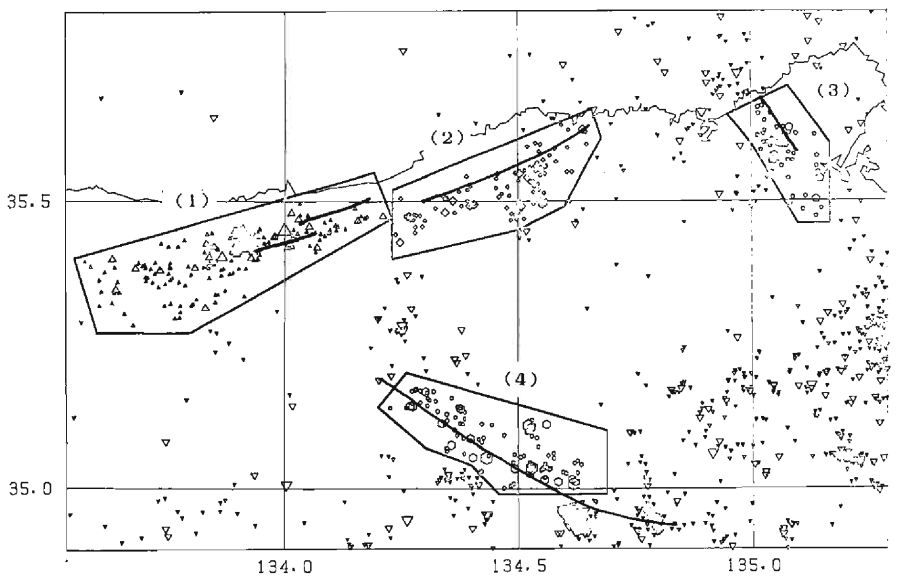

Fig. 65 Epicentral distribution of microearthquakes from June, 1964 to March, 1985 observed by the Tottori Microearthquake Observatory. Microseismicities in four regions (1 to 4) are investigated.

Fig. 65 shows the epicentral distribution of shallow microearthquakes ($H<20$ km), especially along the Shikano (1), the Yumura (2), the Gomura (3) and the Yamasaki (4) fault areas, observed by the Tottori Microearthquake Observatory from June, 1964 to March, 1985. Monthly distributions of shallow earthquakes in the four areas shown in Fig. 65 have been calculated using the data from June 1976 to May 1982 in which the level of seismicity was comparatively low throughout the whole region. The result was then compared with that from June, 1964 to May, 1976 reported by Oike (1977)[5].

In the Gomura fault area (3), where microseismicity is generally low, monthly distribution of earthquakes including smaller ones ($M\geqq 2$) has its highest peak in May, as shown in **Fig. 66**. The corresponding monthly distributions in the Yamasaki fault area (4) and the west Tottori area (1), including the Shikano fault, where the seismicity is comparatively high, are shown in the same figure. The distribution in three fault areas for two periods mentioned above are shown for the sake of comparison. They have peaks in March or September similar to the result in **Fig. 63**. **Fig. 67** shows the total monthly distribution of earthquakes with magnitudes greater than or equal to 3.0 over the four active fault regions from June, 1964 to May, 1983, excluding the most active period after 1983. It indicates the same pattern as that from the JMA data by Ogata (1983)[17] shown in **Fig. 63**.

The largest shock which occurred in this region since 1964 was a M 6.2 earthquake on October 31, 1983 in the central part of Tottori prefecture. **Fig. 68** shows the change of daily precipitation before and after this main shock. The figure

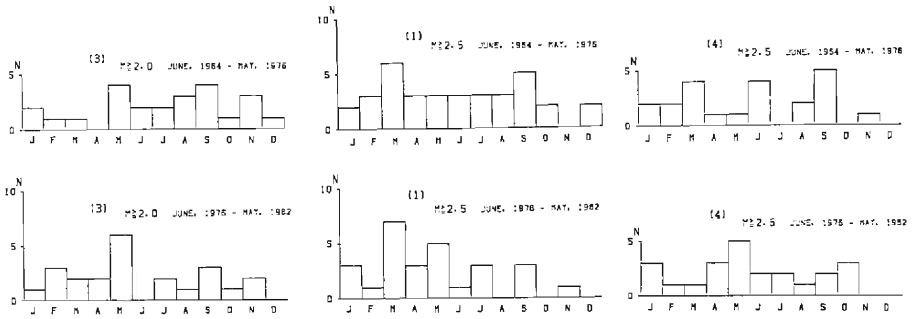

Fig. 66 Examples of monthly distribution of microearthquakes in the Shikano (1), Gomura (3) and Yamasaki (4) fault regions. Region numbers are indicated in Fig. 65.

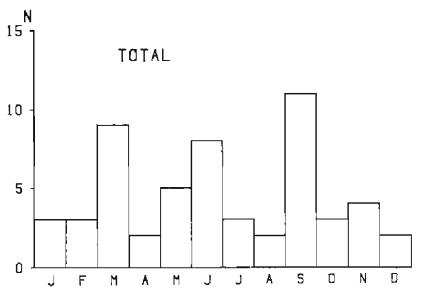

Fig. 67 Monthly distribution of earthquakes ($M \geqq 3.0$) from June, 1964 to May, 1983 in four active fault regions.

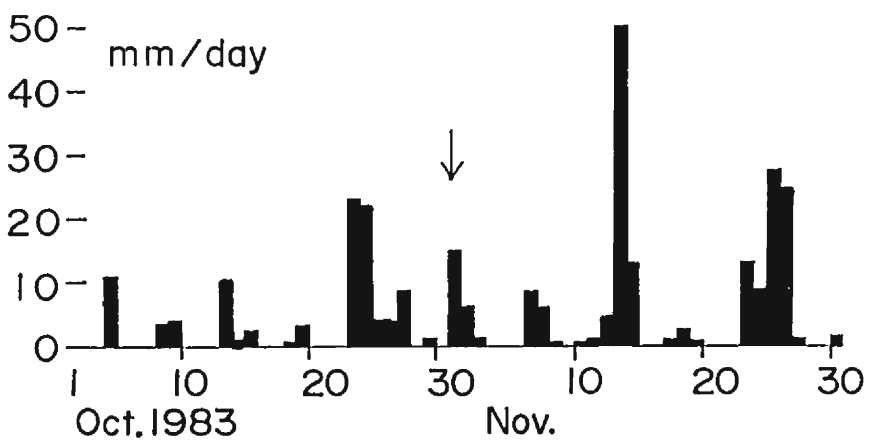

Fig. 68 Daily precipitation before and after the recent largest event ($M=6.2$) in the Tottori prefecture.

shows that heavy rainfall was observed just before the main shock of M 6.2.

Fig. 69 shows the monthly distribution of earthquakes throughout the whole region as shown in **Fig. 65** from June, 1964 to May, 1983. The earthquakes which

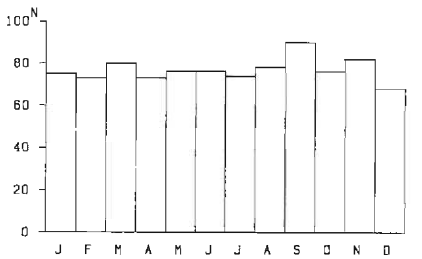

Fig. 69 Monthly distribution of earthquakes in the whole region as shown in Fig. 65 from June, 1964 to May, 1983. Earthquakes occurring within 5 days after the previous one were not counted.

occurred within 5 days after a previous one were not counted. No seasonal characteristics were found in this distribution, even if there are weak peaks in March and September as shown in **Fig. 67**.

The results in this chapter suggest that there appears to be a close relation between the seismic activity including small earthquakes and rainfall in the active fault regions.

6-2. The Outer Zone of Southwest Japan

The Outer Zone of Southwest Japan is the most active region where great earthquakes with magnitudes larger than 8 have frequently occurred. Eleven great earthquakes with magnitudes over 7.8 have occurred along the Nankai trough in this region since A.D. 416. Some of them occurred just a few years after a previous one.

This nature is similar to that described in the previous section on the Inner Zone seismicity. Existence of such a nature as successive occurrence in the neighboring regions means that the stress level just before the occurrence of the latter shock was under critical condition. Under such conditions various kinds of triggers will act effectively to induce large earthquakes.

Fig. 70 shows the space-time plots of large earthquakes along the Nankai trough.

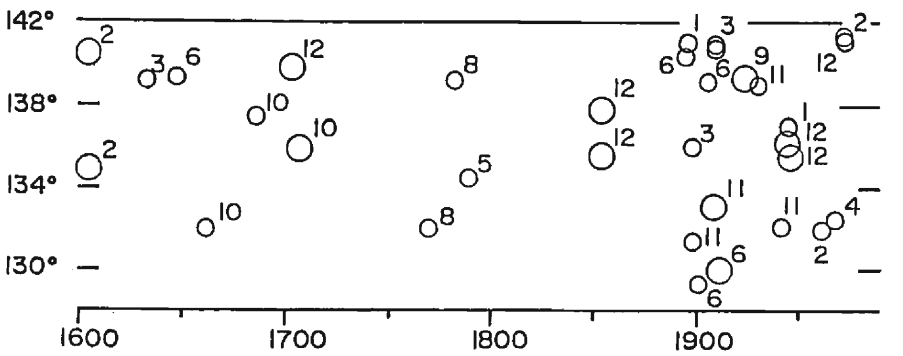

Fig. 70 Space-time plots of large earthquakes along the Nankai trough. Numbers shows the month of the occurrence of shocks.

The numbers in the figure show the months of occurrence of plotted shocks. This shows that seasonality and a nature of successive occurrence of earthquakes have been found in this region.

7. Discussions

In such a problem as the present study treating with systematic and quantitative analyses on seasonality of earthquake occurrence, needless to say, it is important to adopt fully qualified data and the most suitable method. First, the five catalogues used in the present study, namely, the NOAA's catalogue, the historical data set in China, the historical earthquake list in Korea, the list of disastrous earthquakes in Japan, and the list of microearthquakes in Southwest Japan, all described in detail in Chapter 2, may be considered fully homogeneous and of long-term and therefore qualified for the purpose of this analysis.

It is also important to select the most suitable manner for division of an earthquake region into smaller seismic areas in which seasonality can be mutually compared. As to this problem, tectonic conditions and epicentral distributions were mainly considered and then rearrangement of seismic areas was made, if necessary.

The problem of periodicity of such a point process as time-series of earthquake occurrence will be most properly solved by Ogata's point process model. Therefore, this method was applied to a total of 96 seismic areas in the world, in order to clarify the periodic nature of earthquake occurrence in each area.

As the result of the above procedures of analysis, it is considered valid to investigate statistically these global data on the same criterion.

Since so many pages would be needed to present all the graphs of analyses for all 96 areas, only a limited number of graphs were shown in **Fig. 3, 5, 12, 18, 22, 27, 28, 29, 37, 38, 42, 48, 49, 51, 58** and **62** for typical examples. The tables of

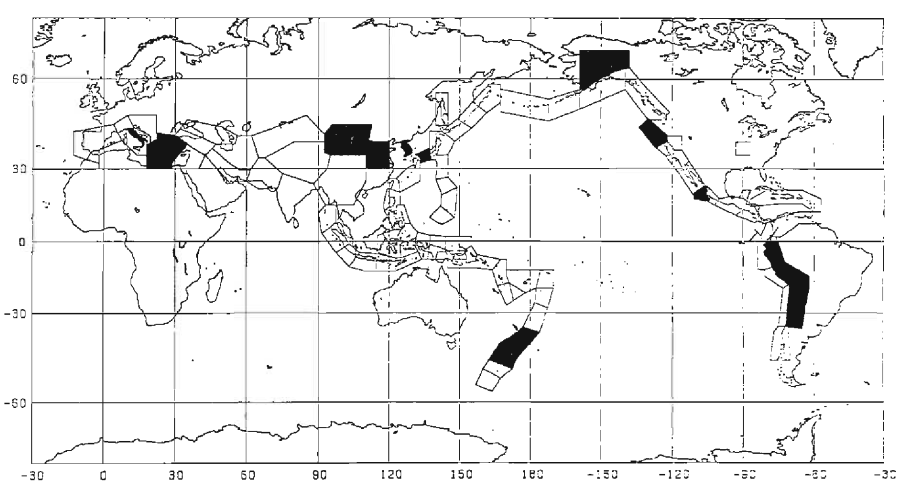

Fig. 71 The areas where seasonality has been shown to exist by this analysis.

AIC of these ares are shown in **Table 1** to **5** and **Appendix**.

Various results of this analysis will be discussed in the following sections.

7.1 The area where seasonality was detected.

(a) Alaska (A4),
Continental South America,
New Zealand (F2, F3 and F4),
Inner Zone of Southwest Japan (J6),
Northeast China and Korea Peninsula,
Italy,

(b) Mississippi River (B6),
Central China (L1),

(c) North part off the West Coast of USA (B1),
West Coast of Central Mexico (C1),
Outer Zone of Southwest Japan (J4),
Aegean Sea (N2 and N3).

In group (a) seasonality was remarkable. Two areas of group (b) show seasonality although it is somewhat vague compared with that of group (a).

Seasonal variations in Northeast China and the Korean peninsula were more clearly observed in the historical data than in present data by NOAA.

Areas in group (a) and (b) are all situated inland. On the other hand, four areas in group (c) are located in oceanic regions.

7.2 Characteristics of the above seismic areas with seasonality

We can point out some characteristics common to these areas as follows:

(a) These areas are located in the middle latitude zones from 20° to 50°N or S, as shown in **Fig. 71**.

(b) The areas in group (a) which show clear seasonality are all located in intraplate regions just behind active interplate seismic regions. Generally, many active faults exist in these intraplate areas.

(c) Seismic activities in these intraplate areas are generally not so high compared with adjacent regions. In China, for instance, seasonal variation has been observed in the northeastern parts where the seismic activity is relatively low.

(d) Conversely, seasonal variation of seismic activity was not observed in either tropical and oceanic areas, as shown in **Fig. 71**.

7.3 Some relations between seasonality of seismic activity and meteorological phenomena, mainly precipitation and temperature.

Natural phenomena which indicate seasonal variation are mainly meteorological ones. Therefore, the seasonal variation of seismic activity was compared with meteorological variations such as precipitation in Chapters 4 to 6.

In all of the intraplate areas in the above noted group (a), the pattern of varia-

tion of seismic activity was found to be similar to that of precipitation or the rate of change of precipitation in respective areas.

In group (a), the patterns of seasonal components are quite similar to that of the distribution of monthly mean precipitation. The peaks correspond to that of the change rate of precipitation in the Alaska area, continental South America and Italy. In continental South America, there are two seasonal component peaks and each corresponds to that of change rate of monthly mean precipitation along the coast or in a mountain district. In New Zealand, the peaks of seismic activities in three areas where the seasonalities exist are a little different from one another. But in N3 area where almost all earthquakes occurred inland, the peak of seismicity corresponds to the peak of the change rate of precipitation in Wellington within this area. In the Inner Zone of Southwest Japan, the best fitting model by NOAA's data has only one peak of seasonal components. Then the correlation between seismicity and precipitation is not so clear but the peak of seasonal components corresponds to the wet season. It was shown that the peak of seismicity corresponds to that of the change rate of precipitation by analyzing microearthquake data. By analyzing historical data, it was found that in the eastern part of China the peak of seismicity corresponds to that of the change rate of precipitation, and in Korea it corresponds to the peak of precipitation.

As for group (b), in the B6 area along the Mississippi river, there is not enough data of earthquake to analyze by statistical methods, but the peak of its distribution corresponds to that of precipitation. In this area, the ascent of water level of the Mississippi river might be considered to be related to seismic activities. In the central part of China including desert areas over an extensive region, we cannot find such relations as above. But in this region the peak of earthquake activity corresponds to the flood season of big rivers.

In every area of group (a), the peak of seismicity lies between the beginning of the wet season and the midst of it. This may suggest that permeation of groundwater by rainfall in the beginning of the wet season could act as an effective trigger to the occurrence of earthquakes and the peak of seismicity appears just after that season. The time lag from the peak in the change rate of precipitation to that of seismicity may depend upon the conditions of the stress field and structures in the crust. The investigation on the relations between permeation process of groundwater and the conditions of the stress field in the various seismic regions would be necessary for further studies.

On the other hand, in group (c), the oceanic area with seasonality of seismicity, we naturally can not find correlation with precipitation there. However, amplitude of annual variation of temperature in these areas is larger than that in tropical areas.

7.4 Some considerations on the mechanisms of earthquake occurrence and its seasonal variation.

As stated earlier, the areas in group (a) are situated in the intraplate region

just behind the active interplate seismic zone, and have not such high seismic activity. If tectonic stress in the crust in such areas becomes somehow critical, meteorological phenomena such as precipitation itself or its rate of change may act as a trigger to earthquake occurrence. This is because the amplitudes of rainfall and temperature largely change from season to season in the middle latitude region. On the other hand, such triggering effects may not be found in active seismic regions, and also not in tropical regions.

As indicated by the induced earthquake phenomena mentioned in the introduction, the effect of groundwater on earthquake occurrence may be considerable in a critical stress state. This is considered to be caused by permeation of groundwater into cracks of rock and decrease in the strength of the rock. Our results suggest that the triggering effects to the occurrence of earthquakes by groundwater appears from a few days to a few months after heavy rainfalls. Existence of many active faults in the intraplate seismic region just behind an active interplate seismic region, as seen in the areas of group (a), may promote the effect of groundwater mentioned above.

8. Conclusions

(1) Through analysis using the world wide data set, it has been found that the regions where seasonal variation of seismic activity, mainly annual and semi-annual periodicities, were determined had systematic features.

(2) The areas where the seasonal variations were found were as follows:

(a) Alaska,
(b) Continental South America,
(c) New Zealand,
(d) Inner Zone of Southwest Japan,
(e) Northeast China,
(f) Korean Peninsula,
(g) Italy,
(h) North part of the West Coast of USA,
(i) West Coast of Central Mexico,
(j) Outer Zone of Southwest Japan,
(k) Aegean Sea.

All of these areas are located in the middle latutide zone. The areas (a) to (g) are located in the intraplate seismic region just behind the active interplate seismic zone and seismic activities are generally low there. The areas (h) to (k) are situated in the middle latitude oceanic zone.

(3) Conversely, no seasonalities of seismic activity were found in the tropical and oceanic regions.

(4) Correlations between seasonal variation of seismic activity and variations of precipitation and of its change rate were high in the middle latitude zone because

of its clear seasonality. This phenomenon was explained by a triggering effect of groundwater which penetrated into cracks of the crustal rocks. Moreover, such a trigger is considered to act effectively in the comparative low seismic regions.

(5) These results on seasonality of earthquake occurrence may give important information to clarify the mechanism of earthquake occurrence and also may be useful for earthquake prediction studies.

Acknowledgments

The author is grateful to Prof. Y. Kishimoto for critical reading of the manuscript and his encouragement in carrying out this work. The author thanks Dr. K. Oike for valuable discussion throughout the study. The author has benefited greatly from discussion with Dr. Y. Ogata and also from his critical advice to the manuscript. This work was enabled by his program in TIMSAC84 (Time Series Analysis and Control Program Package). The author thanks Prof. Zhu Chuan-Zhen of the Institute of Geophysics of the Chinese Academy for preparation of precipitation data in China. The author indebted to Miss E. Fujimoto for completing the manuscript. The data processing was run on a FACOM M340R at the Information Data Processing Center for Disaster Prevention Research, Disaster Prevention Research Institute, Kyoto University.

Appendix

Tables of AIC for the areas whose monthly distributions of earthquakes are shown in this paper.

A1 AREA

K \ J	0	1	2	3	4
0	947.44	929.96	930.30	914.32	916.28
1	961.52	933.18	933.57	917.58	919.22
2	963.50	935.90	936.60	921.24	923.15

A3 AREA

K \ J	0	1	2	3	4
0	930.54	931.12	931.91	933.41	935.33
1	934.02	934.54	935.07	936.43	938.35
2	937.12	938.25	938.50	939.78	941.71

B1 AREA

K \ J	0	1	2	3	4
0	573.79	574.62	575.99	577.97	579.66
1	573.49	572.84	574.57	575.97	577.95
2	576.11	575.96	577.86	579.45	581.32

B4 AREA

K \ J	0	1	2	3	4
0	436.72	438.53	440.22	442.18	440.63
1	437.89	439.85	441.71	443.44	441.54
2	440.83	442.75	444.29	446.27	445.37

B6 AREA

K \ J	0	1	2	3	4
0	243.87	245.00	246.25	245.97	246.93
1	244.08	244.00	245.35	246.93	247.79
2	247.85	247.94	249.28	250.88	251.78

C1 AREA

K \ J	0	1	2	3	4
0	867.80	858.59	859.69	861.12	859.41
1	861.28	854.38	855.36	856.14	856.02
2	862.04	857.97	857.67	858.84	859.01

C5 AREA

K \ J	0	1	2	3	4
0	686.21	687.90	689.27	690.51	689.34
1	688.63	690.29	692.02	693.79	692.25
2	690.00	691.75	693.72	695.64	692.35

D2 AREA

K \ J	0	1	2	3	4
0	598.66	599.04	600.73	602.71	604.69
1	599.41	599.66	601.66	603.58	605.36
2	601.80	602.07	604.00	605.95	607.65

E1 AREA

K \ J	0	1	2	3	4
0	488.88	474.56	469.38	469.23	471.21
1	490.98	476.56	471.72	473.15	475.09
2	493.11	480.01	474.94	476.57	478.42

E3 AREA

K \ J	0	1	2	3	4
0	448.90	435.52	419.01	421.01	423.00
1	448.59	435.11	422.93	424.38	426.41
2	449.07	436.64	426.83	428.35	430.32

E6 AREA

K \ J	0	1	2	3	4
0	692.45	682.77	684.70	686.70	688.69
1	693.48	683.30	685.20	687.16	689.11
2	690.46	685.64	686.56	688.52	690.48

E7 AREA

K \ J	0	1	2	3	4
0	824.26	784.82	753.96	754.67	756.13
1	825.07	787.87	757.08	757.44	758.32
2	821.73	790.90	759.60	759.26	759.21

OCEAN REGION OF SOUTH AMERICA

K \ J	0	1	2	3	4
0	764.91	752.23	753.71	753.65	755.63
1	767.15	755.71	757.17	756.45	758.23
2	771.11	759.21	760.91	760.40	762.23

F1 AREA

K \ J	0	1	2	3	4
0	1036.54	1017.35	1019.35	1016.87	1017.12
1	1036.69	1018.97	1020.68	1018.53	1019.21
2	1039.28	1021.13	1022.73	1020.51	1022.32

F2 AREA

K \ J	0	1	2	3	4
0	491.10	492.87	493.87	495.75	494.83
1	488.79	490.61	491.16	492.72	491.98
2	490.13	492.09	492.71	494.29	493.70

F3 AREA

K \ J	0	1	2	3	4
0	244.13	244.01	243.14	242.78	242.79
1	241.45	242.75	243.69	245.64	245.93
2	245.02	246.43	247.27	248.76	248.54

F4 AREA

K \ J	0	1	2	3	4
0	340.66	339.55	341.55	343.01	344.78
1	339.47	339.01	340.58	342.16	344.09
2	339.61	341.40	343.30	345.21	347.15

F5 AREA

K \ J	0	1	2	3	4
0	341.23	341.65	343.24	345.24	345.46
1	343.29	344.35	346.07	348.04	348.43
2	342.05	342.98	344.01	345.76	345.68

F6 AREA

K \ J	0	1	2	3	4
0	340.02	337.40	323.68	325.68	327.68
1	343.85	338.47	327.66	329.56	331.55
2	346.47	340.84	331.63	333.54	335.53

G2 AREA

K \ J	0	1	2	3	4
0	1106.39	1051.14	1029.98	1031.96	1031.99
1	1110.00	1053.75	1049.74	1035.61	1035.98
2	1112.92	1056.78	1043.83	1038.96	1039.62

H1 AREA

K \ J	0	1	2	3	4
0	943.63	917.68	915.17	909.53	911.51
1	946.90	921.55	918.53	913.08	915.04
2	949.60	924.72	921.64	915.83	917.83

H2 AREA

K \ J	0	1	2	3	4
0	1157.88	1129.59	1128.25	1128.02	1129.52
1	1161.37	1130.95	1130.15	1129.54	1131.07
2	1164.90	1134.60	1133.93	1133.31	1134.87

I3 AREA

K \ J	0	1	2	3	4
0	713.64	699.77	687.41	686.47	688.36
1	717.37	703.72	687.59	686.49	688.47
2	720.89	707.57	690.23	689.98	691.57

J1 AREA

K \ J	0	1	2	3	4
0	827.35	822.16	819.93	816.97	818.32
1	830.60	825.78	823.33	819.80	821.24
2	832.64	827.21	824.67	821.70	823.39

J4 AREA

K \ J	0	1	2	3	4
0	261.12	262.30	263.95	265.28	258.83
1	257.02	258.74	260.60	262.59	261.41
2	259.39	261.26	263.20	265.12	264.42

J5 AREA

K \ J	0	1	2	3	4
0	608.31	594.91	587.91	587.80	584.85
1	605.29	594.40	589.27	591.04	588.82
2	608.18	598.18	592.84	594.65	592.57

J6 AREA

K \ J	0	1	2	3	4
0	317.58	316.41	316.99	318.45	318.70
1	311.69	312.87	314.03	316.01	317.95
2	313.38	315.38	317.38	319.21	321.17

J7 AREA

K \ J	0	1	2	3	4
0	714.17	691.42	688.65	690.14	686.45
1	717.35	694.22	691.36	692.97	688.31
2	721.24	697.36	693.53	695.20	691.61

J10 AREA

K \ J	0	1	2	3	4
0	807.25	776.99	758.07	753.83	755.66
1	810.97	778.81	759.22	755.24	756.46
2	812.36	782.42	762.46	758.75	760.41

J11 AREA

K \ J	0	1	2	3	4
0	840.34	839.51	836.39	836.16	837.49
1	842.84	841.97	838.06	838.47	839.33
2	843.70	841.99	838.85	839.87	841.06

J12 AREA

K \ J	0	1	2	3	4
0	556.38	558.00	554.76	556.62	546.37
1	559.19	560.93	557.32	559.12	550.30
2	561.57	563.48	560.95	562.87	554.16

K1 AREA

K \ J	0	1	2	3	4
0	428.63	415.59	401.64	403.63	404.77
1	432.17	418.62	405.62	407.42	408.07
2	434.14	421.82	409.60	411.39	412.06

L1 AREA

K \ J	0	1	2	3	4
0	488.64	490.62	492.40	493.44	495.43
1	487.86	488.93	490.84	491.60	492.92
2	489.65	491.28	493.25	494.42	496.10

M1 AREA

K \ J	0	1	2	3	4
0	1106.23	1086.69	1063.65	1063.69	1062.81
1	1110.23	1089.81	1066.82	1066.67	1065.38
2	1113.54	1091.19	1070.67	1070.60	1069.25

M2 AREA

K \ J	0	1	2	3	4
0	998.44	979.46	974.28	974.26	973.64
1	1000.80	982.10	977.63	976.93	976.33
2	1003.58	985.39	979.88	979.05	978.36

M3 AREA

K \ J	0	1	2	3	4
0	332.98	333.13	330.87	332.71	334.70
1	335.62	336.30	334.74	336.66	338.61
2	335.60	336.75	335.40	337.29	339.23

M4 AREA

K \ J	0	1	2	3	4
0	566.72	568.45	569.72	570.70	571.00
1	568.24	569.26	570.11	571.07	570.79
2	570.90	572.03	572.45	573.33	574.09

M5 AREA

K \ J	0	1	2	3	4
0	604.85	601.88	594.22	592.83	594.65
1	608.82	605.66	598.17	596.62	598.32
2	612.51	609.65	602.10	600.51	602.21

N2 AREA

K \ J	0	1	2	3	4
0	422.65	421.03	422.53	422.81	423.41
1	419.71	[419.20]	421.16	422.37	424.14
2	423.04	423.18	425.15	426.32	428.09

N3 AREA

K \ J	0	1	2	3	4
0	371.41	372.34	373.33	375.21	372.40
1	371.52	372.78	374.53	376.43	374.13
2	[369.98]	370.27	371.58	373.53	373.74

ITALY

K \ J	0	1	2	3	4
0	418.68	411.05	402.20	400.37	400.97
1	418.06	411.06	400.65	[398.24]	399.24
2	421.42	412.49	401.67	398.59	399.39

NORTHEAST OF CHINA

K \ J	0	1	2	3	4
0	501.30	503.27	505.14	505.87	505.34
1	[500.27]	501.08	502.72	504.44	504.66
2	501.43	502.70	503.53	505.08	505.30

KOREAN PENINSULA

K \ J	0	1	2	3	4
0	522.70	524.07	523.69	525.53	525.10
1	514.27	514.15	515.73	516.64	[511.96]
2	516.48	517.60	519.37	520.54	515.87

Reference

1) Tributsch, H.: Wenn die Schlangen Erwachen (translated in Japanese), Asahi Shinbunsha, 1978, pp. 1–22.
2) Omori, F.: Annual and Diurnal Variation of Seismic Frequency in Japan, Pub. Earthq. Inv. Comm., 8, 1902, pp. 1–94.
3) Davison, C.: The Annual Periodicity of Earthquakes, Bull. Seism. Soc. Amer., 18, 1928, pp. 246–266.
4) Mogi, K.: Monthly Distribution of Large Earthquakes in Japan, Bull. Earthq. Res. Inst., Vol. 47, 1969, pp. 419–427 (in Japanese).
5) Oike, K.: On the Relation between Rainfall and the Occurrence of Earthquakes, Disas. Prev. Inst. Kyoto Univ. Annuals, No. 20B–1, 1977, pp. 35–45 (in Japanese).
6) McGinnis, L.D.: Earthquakes and Crustal Movement as Related to Water Load in the Mississippi Valley Region, Illinois State Geol. Survey Circular, No. 344, 1963, pp. 1–20.
7) Ozawa, I.: Observation of the Crustal Strains at the Time of Earthquakes around Kyoto City, Spec. Contr. Geophys. Inst. Kyoto Univ., No. 8, 1968, pp. 91–108.
8) Ozawa, I.: Observations of Crustal Deformations in the Periods of the Earthquakes at Kami-Wachi and Kyoto City, Disas. Prev. Inst. Kyoto Univ. Annuals, No. 12A, 1968, pp. 123–136 (in Japanese).
9) Yamauchi, T., M. Yamada and T. Okuda: Earthquake Occurrence and Abnormal Strain Response to Rainfall, Zisin, Vol. 34. No. 3, 1981, pp. 301–310 (in Japanese).
10) Carder, D.S.: Seismic Investigations in the Boulder Dam Area, 1940–1944, and the Influence of Reservoir Loading of Earthquake Activity, BSSA, Vol. 35, 1945, pp. 175–192.
11) Talwani, P.: Earthquakes Associated with the Clark Hill Reservoir, South Carolina —A Case of Induced Seismicity, Engineering Geology, Vol. 10, 1976.
12) Gupta, H.K. and B.K. Rastogi: Dams and Earthquakes, Elsevier, 1976, pp. 1–229.
13) Simpson, D.W., S.K. Negmatullaef: Induced Seismicity at Nurek Reservoir, Tadjikistan, USSR, BSSA, Vol. 71, No. 5, 1981, pp. 1561–1586.
14) Keith, C.M., D.W. Simpson, and O.V. Soboleva: Induced Seismicity and Style of Deformation at Nurek Reservoir, Tadjik SSR, JGR, Vol. 87, No. B6, 1982, pp. 4609–4624.
15) Oike, K. and Y. Ishikawa: Induced Earthquakes associated with Large Reservoirs in China, Chinese Geophysics, Vol. 2, No. 2, 1983, pp. 383–403.
16) Ohtake, M.: Seismic Activity Induced by Water Injection at Matsushiro Japan, J. Phys. Earth, 22, 1974, pp. 163–176.
17) Ogata, Y.: Likelihood Analysis of Point Process and Its Application to Seismological Data, Bulletin of Institute of International Statistics, Vol. 50, Book2, 1983, pp. 943–961.
18) Ogata, Y. and K. Katsura: Point Process Model with Linearly Parameterized Intensity for the Application to Earthquake Data, Essays in Time Series and Allied Processes, J. Applied Probability, Vol. 23A, 1986, in press.
19) Usami, T.: Shiryo Higai-Jishin Soran, University of Tokyo Press, 1975, pp. 1–327 (in Japanese).
20) Kim, K.D. and Suh, J.H.: A Study on the Characteristics and the Cause of Earthquakes in Korea, J. Korean Inst., Mineral and Mining Engineers, 14, 1977, pp. 240–268.
21) Akaike, H.: A New Look at the Statistical Model Identification, IEEE Transactions on Automatic Control AC-19, 1974, pp. 716–722.
22) Oike, K., K. Matsumura and Y. Ishikawa: Large Earthquakes in the Southwest Japan and Seismicity in the Eastern Asia, Jour. Analytical Researches of Data on Natural Disaster, Vol. 9, 1982, pp. 138–146 (in Japanese).
23) Oike, K.: On the Nature of Seismic Activity in the Eastern Asia, Contri. to the Int. Symp. on continental seismicity and Earthquake Prediction, Beijing, China, 1984, pp. 78–87.
24) Matsumura, K. and K. Oike: Seasonal Characteristic of Earthquake Occurrence in Korea and China, Disas. Prev. Inst. Khoto Univ. Annuals, No. 28B–1, 1985, pp. 185–192 (in Japanese).
25) Oike, K.: On a List of Hypocenters Compiled by the Tottori Microearthquake Observatory, Zisin, Vol. 2, No. 28, 1975, pp. 331–346 (in Japanese).